UNIVERSITÀ DEGLI STUDI DI CATANIA
FACOLTÀ DI INGEGNERIA
Dipartimento di Ingegneria, Elettrica e dei Sistemi Tesi di Dottorato
di Ricerca in Ingegneria Elettronica, Automatica
e del Controllo dei Sistemi Complessi
(XXIII)

Umana Elena

IP^{2}C Transducers for All-Organic Electronic Applications

Coordinatore: Prof. L. Fortuna
Turor: Prof. S. Graziani
Ing. M. La Rosa

To Riccardo

and to my nephew

Contents

Introduction

This work focuses on the integration of polymeric transducers in organic electronics applications. Two research environments have been exploited in order to realize a whole plastic motion transduction system, comprehensive of organic electronic control circuits. This kind of system has a huge potential since the two research environments combine the opportunity to develop low cost application with the possibility to use flexible substrates. A new class of mechanical transducers has been introduced: ionic polymer-polymer composites (IP^2Cs). These devices are realized by using only organic materials and manufactured by low cost processing techniques. They are based on Nafion® membranes covered by organic conductors, like PEDOT:PSS. The investigation on organic technology has allowed to improve the performances of these polymeric transducers having both motion sensing and actuation properties. In detail, their manufacturing processes have been reformulated in order to improve the transduction features and overcome the limitation due to the adopted materials. An in-deep investigation of polymeric devices has allowed the development and implementation of a

first model of polymeric sensor in organic technology.

This research activity, from materials study and characterization for realization of organic thin film transistors (OTFTs) to its modeling in CADENCE environment, has allowed the simulation of different circuits and the design of an embedded system for transduction. The design flow has been followed from schematic and simulation to layout.

Chapter 1 introduces polymeric transducers, their working principle and the procedures for the analysis of their electromechanical proprieties. Chapter 2 gives a brief overview about organic electronics, describing the testing platform developed for the characterization of organic semiconductors. Chapter 3 reports an extensive study about all-organic electromechanical transducers. Different organic conductors for electrodes and two different solvents have been used, in order to overtake the limits imposed by organic materials and intrinsic characteristics of transducer. Chapter 4 describes a new technique for organic conductor deposition in order to enhance electrodes adhesion and to overtake the problems of hydration. In the Chapter 5 an embedded system has been designed combining organic electronics and polymeric transducers. The schematic and layout have been designed in CAD environment for further realization.

1

Ionic Polimer-Polimer Composites

In this chapter a brief introduction on polymeric transducers will be reported. Ionic Polymer-Polymer Composites (IP^2Cs) are a novel class of all-organic electroactive polymers that can operate both as electromechanical actuators and as sensors. They are an evolution of Ionic Polymer-Metal Composites (IPMCs), since the metallic layers, used to realize the electrodes, are substituted by using organic conductors, based on PEDOT:PSS.

1.1 Towards polymeric transducers

In recent years a wide interest has been devoted to the research on innovative materials for the development of flexible electromechanical transducers. More specifically, electroactive polymers (EAPs) have been extensively investigated for their flexibility and lightness. Among these materials, Ionic Polymer-Metal Composites (IPMCs) have been demonstrated to exhibit sensing and actuation capabilities [1, 2, 3, 4].

IPMCs are constituted by an ion exchange perfluorinated membrane (e.g. Nafion®115 or Nafion®117), coated on both sides with a metallic electrode, generally a noble metal (such as platinum or gold). These metals are characterized by high cost and require complex deposition techniques in order to manufacture the electrodes. For these reasons, transducers with electrodes realized by using organic conductors [5], named Ionic Polymer Polymer Composites (IP^2Cs), have been introduced [6][7] and investigated. This new class of all-organic transducers exploits polymers that are becoming available and that are characterized by high conductivity values. They have already attracted researchers' interest in various application domains from electronics to robotics or biochemistry organic conductors. In fact, organic conductors are mainly processable from solutions and allow the use of low-cost deposition techniques such as spin-coating, dip-coating, spin-casting or printing techniques. In detail, the used organic conductor is PEDOT:PSS characterized by a good conductivity (> 100 S/cm) and different types have been synthesized, with increasing conductivity values. Some of them have been employed in order to the electrodes manufacture and to improve performances of devices.These devices present a layer structure as shown in Fig. 1.1: two layers of organic conductor cover the sides of Nafion® membrane.

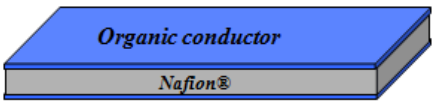

Fig. 1.1. Layer structure of a IP^2C.

1.2 IP^{2}C devices working principle

IP^{2}C actuation and sensing capabilities have been proved and their behavior investigated. In the case of actuator behavior, when a voltage is applied across the membrane thickness, it bends towards the anode side and the bending increases with the amplitude of the applied voltage. The obtained deformation is believed to be the result of two different contributions. The first one is due to the solvent (water or other solvents) molecules transport and is strictly linked to the ions that are free to move inside the polymer net; when an external voltage is applied between the electrodes, the mobile cations, free to move inside the polymer net, move towards the cathode. If the membrane is hydrated, the cations carry with them solvent molecules, in a parasitical way. In this way the membrane cathode side increases its volume, while the anode region decreases its volume and hence contracts. The result is the bending of the strip towards the anode. A second contribution to the membrane deformation, when a voltage is applied, is supposed to depend on the charges distributed on the electrodes and could be due to the Coulombian interactions arising between charges in the organic conductor electrodes and the negative fixed charged groups belonging to the polymer matrix thus it strictly depends on the quality of the deposited electrodes.

The performance of the IP^{2}C transducer can be measured by the unconstrained free deflection of the device tip. The sensing capability has been demonstrated by measuring the inverse performance: the short cir-

cuit current voltage produced by the transducer when a deformation is applied. The relationship between induced current in the polymer results to be proportional to the mechanical deformation. The sensing capability of the device is dependent upon several factors, as such the frequency of the applied bending and the length of the transducer.

1.3 Procedures for experiments on IP^{2}C

The analyses of IP^{2}C electromechanical propriety have required the development of experimental procedures and devices in order to determine transduction features. The analysis of viscoelastic features of used polymer has been performed through the Dynamic mechanical analysis (DMA). Moreover, sensor and actuator behaviors have been studied and analyzed.

1.3.1 Young modulus

The behaviour of materials [8] of low relative mass is usually discussed in terms of two types of ideal materials: the elastic solid and the viscous liquid. The former has a definite shape and is deformed by external forces into a new equilibrium shape; on removal of these forces it reverts to its original form. The solid stores all the energy that it obtains from the external forces during the deformation, and this energy is available to restore the original shape when the forces are removed. By contrast, a viscous liquid has no definite shape and flows irreversibly under the action of external forces. One of the most interesting features of poly-

mers is that a given polymer can display all the intermediate range of properties between an elastic solid and a viscous liquid depending on the temperature and the experimentally chosen time-scale. In detail Young modulus quantifies the elasticity of the polymer, it provides data about ability to deform of a material when a stress is applied to it. It is defined, for small strains, as the ratio of rate of change of stress to strain: $E = \frac{\sigma}{\varepsilon}$.

Young modulus is highly relevant in polymer applications involving the physical properties of polymers. Polymers have usually a viscoelastic behaviour. With low temperature, or high measurement frequencies, polymer can have a glassy behaviour and presents a Young modulus of $10^9 - 10^{10} Nm^{-2}$ and breaks with strain more than 5%. Whereas, with high temperature, or low frequencies, polymer presents characteristics of a rubber and a Young modulus of $10^6 - 10^7 Nm^{-2}$, that can undergo high stretch(about 100%) without permanent strain. In case of middle values of temperature and frequencies (glassy transition range), the polymer behaviour does not exhibit rubber or glass feature and can dissipate, straining, a considerable amount of energy. Dynamic Mechanical Analysis (DMA), is a technique used to study and characterize materials which is most useful for observing the viscoelastic nature of polymers. The experimental procedure consists in subjecting the specimen to an alternating strain and simultaneously measure stress. For linear viscoelastic behaviour, when equilibrium is reached, the stress and strain are expressed by the following equations:

$$\sigma(t) = \sigma(\omega) e^{i\omega t} \tag{1.1}$$

$$\varepsilon(t) = \varepsilon(\omega)e^{i\omega t} \tag{1.2}$$

where ω is the angular frequency. The measures of strain and stress provide complex modulus values $E^*(\omega)$, defined through the followed expression:

$$\frac{\sigma(\omega)}{\varepsilon(\omega)} = E^*(\omega) = E'(\omega) + iE''(\omega) \tag{1.3}$$

where $E'(\omega)$, which is in phase with strain, is called the storage modulus because it defines the energy stored in the specimen due to the applied strain. While $E''(\omega)$, which is $\pi/2$ out of phase with the strain, defines the dissipation of energy and is called the loss modulus, because the energy (ΔE) dissipated per cycle can be computed as:

$$\Delta E = \pi e_0^2 E'' \tag{1.4}$$

The ratio between storage and loss modulus defines the damping factor:

$$tan\delta = \frac{E''}{E'} \tag{1.5}$$

The DMA analysis of IP^{2}C samples has been performed by means of Tritec 2000 DMA produced by Tritec Technology (thanks to the collaboration with DMFCI of Università degli Studi di Catania) shown in Fig. 1.2. A force (stress) is applied to the sample. The stress is transmitted through the drive shaft onto the sample which is mounted in a clamping mechanism.

1.3.2 Characterization experimental setup

The experimental setup has been realized ad hoc in order to characterize the device behavior. In case of actuators, a voltage signal is used to

Fig. 1.2. Tritec 2000 DMA equipment.

deform the membranes, while in case of sensors, a displacement is applied obtaining, a short-circuit current. The scheme of the experimental setup realized for the actuator characterization, including the data acquisition section, shown in Fig. 1.3. A buffer (realized via an OPA548) was needed to deliver the required current which is of the order of hundreds of milliamperes to the actuator, while the instrumentation amplifier (INA111) was used to measure the absorbed current, by using the shunt resistor R_s. The IP^{2}C tip displacement was measured by using a laser distance sensor (Baumer Electric OADM 12). Data were acquired by a National Instruments^{TM} USB-6008 multifunction DAQ card and sent to a computer.

Fig. 1.4 shows two different schemes of setup used to perform the sensor characterization. In detail, Fig. 1.4(a) reports a first measurement setup used to observe sensor operation. In fact, it allows to determine sensing current of a membrane that is strained through a impulsive impact system. The other experimental setup (Fig. 1.4(b)) allows to analyze and determine more information about sensing behavior.

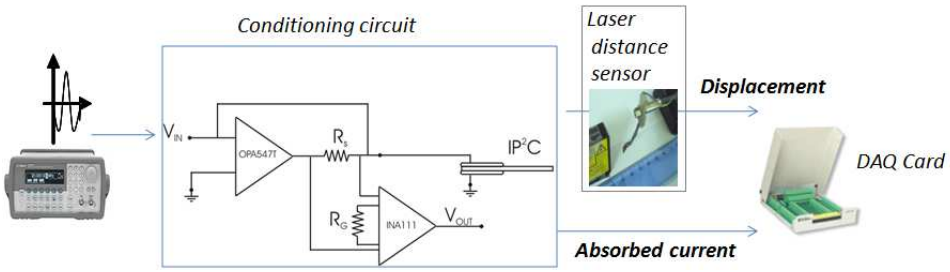

Fig. 1.3. Experimental setup scheme for actuating measurements.

Moreover, it can apply different signals to the vibrating system, in order to observe and analyze membrane behaviour.

In a first phase the electromechanical capabilities of IP^{2}C sensor have been tested using a mechanical apparatus designed to impose the membrane deformation by periodic impulsive impacts, shown in Fig. 1.4(a). It is composed by a moving cylindrical bumper made of plastic, actuated by a CC motor through a gearing system and a slider. The plastic bumper hits the IP^{2}C membrane alternating the face of the impact. The periodic impacts cause a sensing current flowing through the short-circuit amplifier that is acquired by a computer, through a DAQ card. In a second set of experiments , the mechanical stimulus was imposed to the IP^{2}C membrane by means of the programmable mechanical vibration generator system (TIRA Schwingtechnik TV50009) shown in Fig. 1.4(b). The mechanical vibration generator was driven by a voltage signal produced by an arbitrary function generator or directly by a computer, through the DAQ card, in case of a tailored signal. The mechanic wave was transmitted to the membrane through two copper electrodes which are printed inside the clamps. They allow

also to sense the IP^{2}C short-circuit current by means of a high gain current to voltage amplifier based on LF411 operational amplifier (conditioning circuit). At the other side of the strip, a load cell (Transducer Techniques GSO-10) has been used to measure the blocking force. Furthermore, the displacement δ has been measured close to the clamp by using a laser distance sensor (Baumer Electric OADM 12). The signals measured by the current amplifier, the load cell and the laser sensor were recorded by means of a National Instruments USB-6008 multifunction DAQ card. A graphical user interface, developed under Labview^{TM} environment, has been developed in order to drive the multifunction DAQ card. Moreover, it allows to display and make a first analysis of recorded signals. Data were processed by suitable Matlab®scripts that will be described in following chapters.

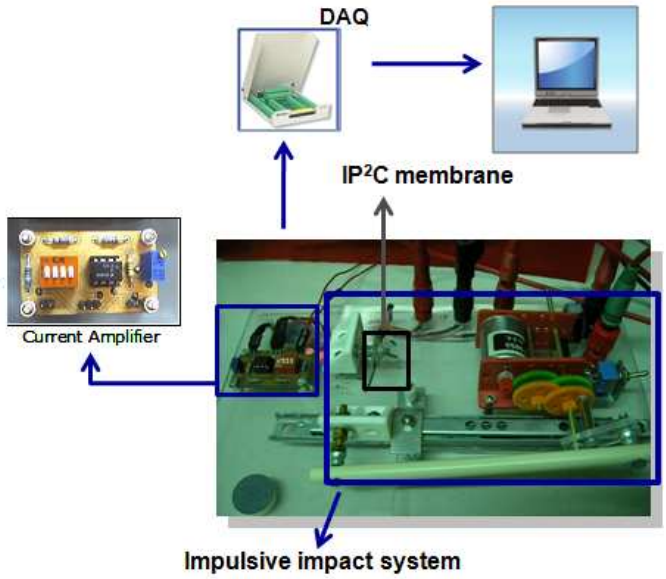

(a)

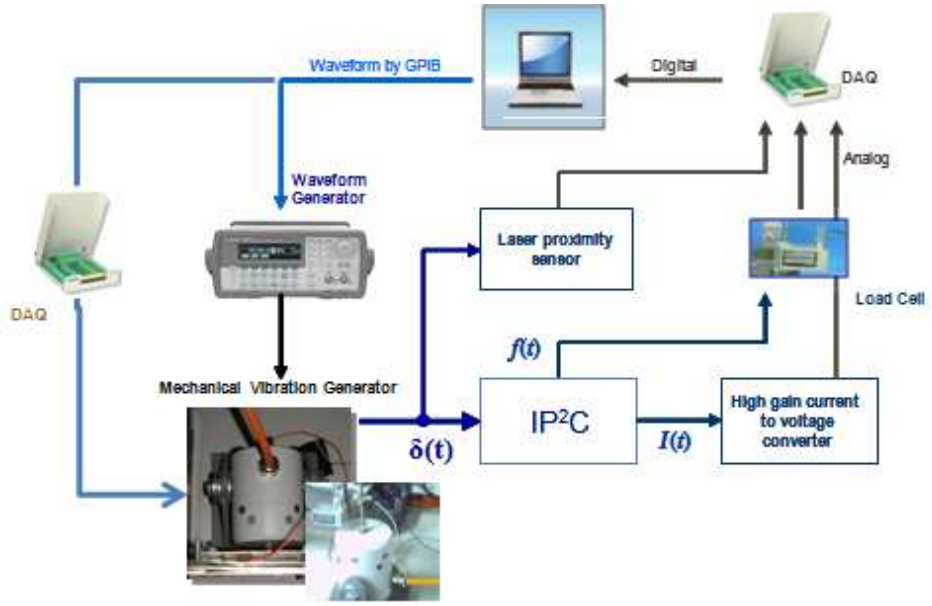

(b)

Fig. 1.4. Experimental setup schemes for sensor measurements.

2

Organic Electronics

The development of post silicon technologies, based on organic materials, consolidates the possibility to realize new devices and applications with unusual properties: e.g. flexibility, light weight, disposability. Both materials and processes play a fundamental role in this new electronic framework and have been improved continuously in the last decades. In this chapter a complete framework for characterization and modeling of organic semiconductor materials is reported [9]. Multifunctional testbeds have been developed to analyze different organic semiconductors through hybrid demonstrators of multilayered structure devices.

2.1 Organic electronics overview

Since the realization of the first Organic Thin Film Transistor in 1983 [10], an intense research effort has been dedicated to both the improvement of organic materials and development of innovative de-

position and manufacturing techniques for low cost electronics assessment. Up to now organic thin film transistors have been investigated for applications in different fields from electronic backplanes in organic light-emitting diodes (OLED) for rollable displays, to chemical and bio-FET sensors, to simple logic circuits, to be associated with radio-frequency identification (RFID) tags, as well as with thin- film batteries and e-paper in new multi-functional systems [11, 12, 13]. Organic material properties have been tailored to obtain required features for electronic applications by designing new molecules with enhanced properties, improved lifetime and environmental stability, as well as solution processability and feasible charge mobility. Thus, the possibility to modify the composition and material preparation is the strongest turn of post silicon technologies in the electronic application field. Thanks to the improvements obtained in recent years, organic semiconductors exhibited charge mobility values comparable to amorphous silicon and polysilicon [14, 15, 16]. On the other hand, stamp-based imprinting processes are going down to tens of nanometers in scale, without the high costs of conventional lithography. Nanoimprint Lithography (NIL) and Soft Lithography (SL) processes [19], [20], based on hard and soft stamps respectively, are continuously improved and equipment manufacturers are investing to realize machineries to manufacture organic devices on large area. Imprinting lithography, combined with low-cost deposition techniques like spin-coating and inkjet printing, are currently adopted to realize multilayered structures of materials processed by solution. The combination of the former aspects, materials and pro-

cess, paves the way to the fabrication of new active and passive devices for advanced applications. In this perspective, a consolidated workflow going from materials to devices is required considering a complete Technology Platform that describes the process flow-chart and the tools used in the design, layout and realization of an organic electronic circuit. The basic elements which define the organic technology platform are: organic materials, manufacturing process techniques and the CAD framework [21]. The fundamental element of organic electronics is the Organic Thin-Film Transistor (OTFT), developed by different organic materials: conductors, dielectrics and semiconductors. Therefore, materials characterization is an important step towards the realization of organic technology devices.

A testing platform has been designed. The behavior of polymer semiconductors has been analyzed through the characterization of single devices such as transistors or logic gates. Moreover, multifunctional testbeds architectures have been designed following the IEEE Standard 1620-2004 "Characterization of Organic Transistors and Materials".

Hybrid organic structures have been adopted to obtain a standard semiconductor polymers benchmarking. The characterization of the organic semiconductors and the related model OTFT have been performed and device parameters extracted [22].

2.2 Testing platform

The adopted testing platforms for organic electronics are hardware/software systems composed by application demonstrators and testbed. The design processes of demonstrator and testbed follows a sequence of steps according to the application definition as reported in Fig. 2.1.

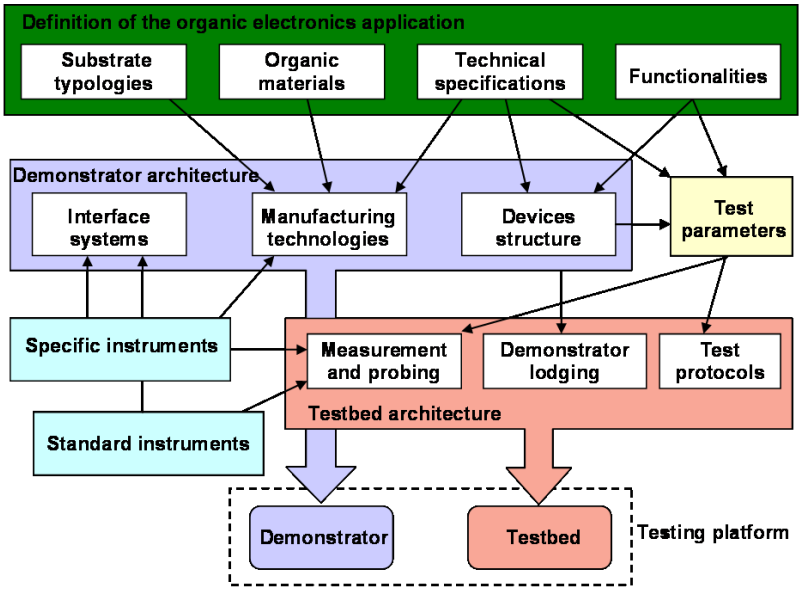

Fig. 2.1. Testing platform design flow. *Copyright [2009]EDP Sciences.*

The application description, by identifying its characterizing elements and its main functionalities, is the first step of the testing platform design.The choice of the application architecture is heavily affected by materials manufacturing techniques. Organic material deposition, synthesis and patterning impose technological limits, to be considered during test platform design. Moreover, any manufacturing technique needs exploiting specifics equipments which influence designing

choices. In this phase technological data (materials, substrate typologies, etc.), operative information (functionalities) and general technical specifics (processing techniques, feature sizes, etc.) are defined. In the next step developed ad hoc demonstrators are described with relative interface systems.

2.3 Materials requirements and processing techniques

Some interesting properties of organic materials such as lightweight, flexibility, ease of manufacturing and low processing costs, motivated an intense research in innovative materials scouting. Organic semiconductors have been extensively studied for long time but only recently they have attracted a more increasing interest, according to the possibility to use them as active layers in Organic Thin Film Transistors. Organic semiconductors can be mainly classified according to the type of charge carriers, which can be holes (p-type) or electrons (n-type). Up to now the lack of feasible electron-transporting n-type materials, which are very sensitive to the environment, hindered the development of organic CMOS technology, thus only p-type materials have been adopted and only ratioed logic p-type circuitries have been designed [23]. The research is actually ongoing toward the improvement of new n-type materials exhibiting highest charge carrier mobility and air stability. Organic semiconductors can also be classified in small molecules and polymers. Among small molecules, oligothiophenes, phthalocyanines, pentacene

and tetracene, generally present good electrical performances, thanks to their high molecular order. However, they are generally insoluble and solution processing techniques cannot be adopted. Evaporation or vacuum deposition process through shadow masks are required with higher costs and higher energies than additive solution manufacturing processes. On the other hand, the class of polymers known as conjugated polymers, characterized by π-conjugated backbone structures containing many double bonds, has shown semiconductor features. Organic semiconductor polymers are of particular interest for innovative applications, being solution processable by very low cost deposition techniques such as spin-coating, dip-coating, or inkjet printing. However, most of these polymers are generally characterized by disordered structures with poorer electrical performances. Nevertheless, the possibility to use solution processing techniques makes them the preferred material for organic electronic development. As concerns the organic conductors, the research in this field has been highly increased since 1977 with the discovering by Shirakawa, MacDiarmid and Heeger for which where awarded in year 2000 with the Nobel Prize in Chemistry. They discovered the ability to dope polymers in the full range from insulator to metal [24]; in particular, they found out that films of polyacetilene (trans-(CH)x), p-doped by treatment with an oxidizing agent such as gaseous bromine or iodine, exhibited an increase in conductivity of many orders of magnitude, passing to a "metallic state". Among available conducting polymers, PEDOT:PSS exhibits the highest conductivity values, i.e. in the order of magnitude of hundreds of siemens

per centimeter. It can be deposited from solution through low cost deposition and patterning techniques such as spin coating, dip coating and various printing techniques such micro Contact Printing (μCP) or inkjet printing. The availability of organic materials with both conducting and semiconducting features paved the way to the development of the organic electronic technology whose primary component is the Organic Thin Film Transistor. In particular, the possibility of manufacturing it through solution and patterning steps in a multilayer functional structure (Fig. 2.2), make them alternative to the traditional inorganic Silicon based electronics. The electric performances are not comparable to the inorganic counterpart but the opportunity to adopt them for realizing economic, large area, innovative applications is highly appealing. The prime key for organic electronic technology development is represented by the availability of a set of organic materials (semiconductors, conductors, dielectrics) with good electrical and chemical characteristics and compatible solvents.

The adopted organic materials must satisfy some requirements which strongly affect the OTFT performances: organic conductors with large conductivities are required for the realization of source and drain contacts; organic semiconductors with high charge carrier mobility and high Ion/Ioff ratio are needed to ensure high current values and low leakages; as concerns the adopted organic dielectric, high-k materials are required as gate dielectrics, while low-k dielectrics are needed as organic insulating materials. Since the interface among gate dielectric and semiconductor is the active area where charge transport takes place, the

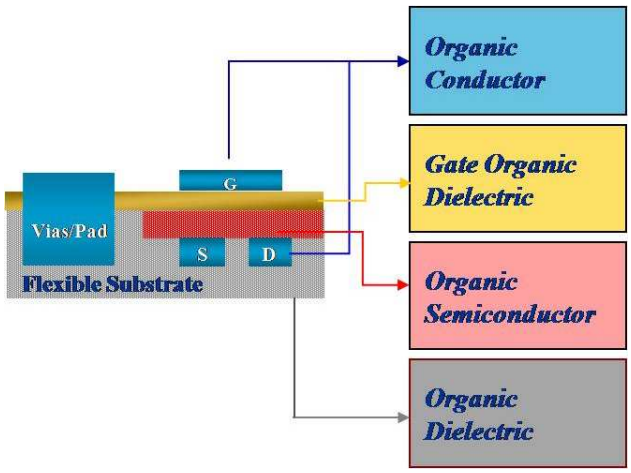

Fig. 2.2. Multilayer functional structure of OTFT and interconnections.

presence of defects act as traps. A semiconductor/dielectric interface with imperfections and an increased roughness implies a decreasing of mobility and device performances. Moreover, the development of post silicon devices based on organic materials implies a deep investigation of the main issues to obtain feasible devices in terms of stability, robustness and efficiency. Many organic materials, such as, e.g., the organic semiconductor Poly3-HexylThiophene (P3HT), have stability problems in air due to the interaction with the external environment and need coating to be protected from oxygen or humidity. Parallel to material scouting, an intense research is also focused on the improvement of deposition and patterning techniques together with large scale manufacturing of flexible organic devices at low cost. In particular, imprinting manufacturing processes, enabling the downscaling of feature sizes, are investigated to guarantee the realization of circuits with the necessary switching speed. Among the imprinting techniques,

two main methodologies can be recognized: the NanoImprint Lithography (NIL) techniques and the Soft Lithographic (SL) ones. These techniques are both based on an imprinting process: NIL process uses an hard stamp generally made in Silicon or UV transparent quartz with feature sizes down to tens of nanometers; the Soft Lithographic process makes use of a soft stamp of poly(dimethylsiloxane) (PDMS) which limits the minimum feature size achievable to hundreds of nanometers. Hard moulds with patterned relief structures are used in both NIL and SL techniques. Moulds are fabricated by conventional processes (optical lithography, e-beam lithography, dry and wet etching, etc.) and can be used many times to produce soft stamps or to pattern directly polymer films. Detachment of patterned films is made possible by anti-sticking treatments of molds [25]. The Fig. 2.3 reports molds master in silicon wafer, with minimum feature size of 200 nm, used for NIL.

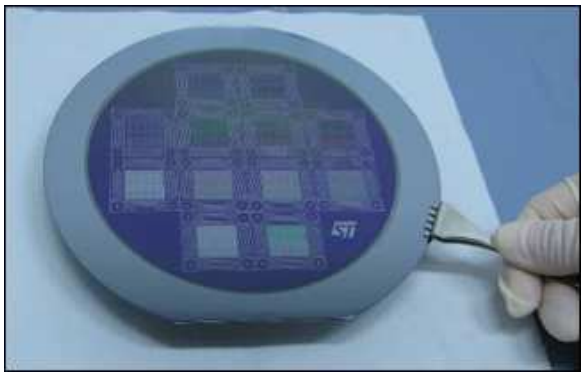

Fig. 2.3. Molds master in silicon wafer.

The manufacturing of a soft stamp is performed by pouring the PDMS over the hard mould, degassing of the poured PDMS in air, cur-

Fig. 2.4. Flexible mold PDMS replica.

ing in oven and finally by peeling-off. The PDMS stamp replicates the silicon mould structures, as shown in Fig. 2.4. Several PDMS stamps can be obtained from silicon moulds thus decreasing the cost related to imprinting manufacturing. The selection between hard and soft stamp patterning is strictly related to the employed materials and the desired geometric feature size. More in details, the NIL technique allows obtaining smaller feature sizes, by using different types of patterning methods: Hot Embossing and UV-Based. The first applies high pressure and heats the material with temperatures higher than the glass transition temperature Tg of the adopted material. The second is used for organic materials curable by UV radiation.

2.4 Demonstrator

Demonstrators based on metallic contacts with a silicon substrate have been used to obtain templates for organic semiconductors testing. Used

demonstrator architectures are thin film transistor (Fig. 2.5(a)) and logic gate(Fig. 2.5(b)) with different feature sizes.

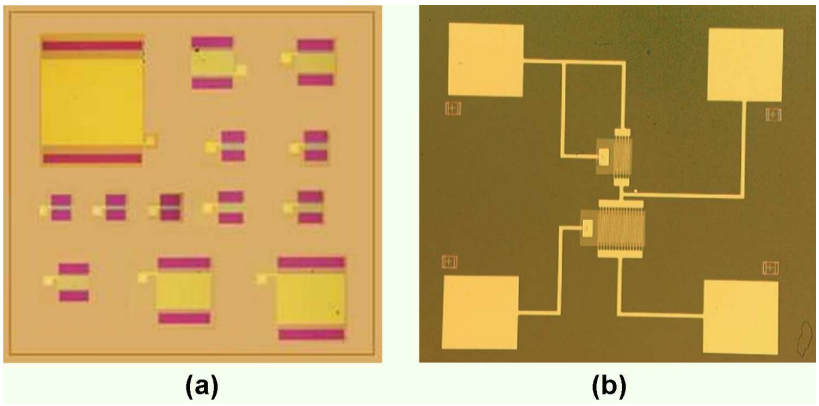

Fig. 2.5. Template of pseudo-pmos organic TFT(a) and inverter(b). *Copyright [2009]EDP Sciences.*

In order to investigate the device behavior different geometrical parameters (such as the channel length and the gate dielectric thickness) have been considered. These structures allow the deposition of different organic semiconductor to be tested. Pads and via interconnections have been designed for guaranteeing the electrical contacts with the characterization equipment by means of a probing system. Logic gates have been designed adopting a conventional pseudo-pMOS architecture which uses only p-type organic transistors. These configurations are mainly constituted by a driver circuit implementing the logic function and a load circuit usually constituted by a transistor operating in the saturation region. Once the application architecture design is completely developed, its validation becomes essential; for

this reason it is necessary the development of multifunctional testbeds. Testbeds are software/hardware systems able to interact with demonstrator samples, designed to implement a set of test protocols. Testbed architecture design can be accomplished through the identification of a set of test parameters. Three main components define the testbed architecture: test protocols, measurement/probing instruments and data lodging systems.

2.5 Testbed architecture

The testing parameters have been defined through the specification of different measurements. The gate leakage curves (I_{GS} vs V_{GS} and I_{GD} vs V_{GD}) characterize the gate dielectric quality and quantify leakage current from the gate to the channel. Leakage measurements are carried out to ensure gate dielectric integrity before subsequent measurements are performed. The transfer curves (I_{DS} vs V_{GS}) allow the preliminary determination of field-effect mobility (μ) and threshold voltage (V_T). The output curves (I_{DS} vs V_{DS}) provide saturation and OTFT electrical performance information and are used to determine whether the device exhibits FET-like behaviour. The capacitance curves (C_{GD} vs V_{GS} and C_{GS} vs V_{GS}) are obtained by the sum of two capacitive contributes: the gate to channel capacitance and the stray capacitance. The stray capacitance values (due to geometrical overlapping of drain source contacts with gate plate) have a negative effect on device switching speed and may affect device electrical characterization. In order to

obtain the required set of measurements, a dedicated multifunctional system, comprising probing, measuring and lodging instruments, has been implemented.

2.5.1 DC parameters of OTFT compact model

A specific strategy has been defined to extract OTFT parameters using electrical measurements. A compact model of organic transistors and a complete characterization of the organic semiconductor have been obtained. The method consists of a differential analysis of the transfer characteristic curves (I_D vs V_{GS}) and exploits the different functional dependencies of current on gate voltage which is induced by the presence of contact resistances. Using the expression of drain current in the linear regime:

$$I_D = K(V_{GS} - V_T)^{\gamma+1} V_{DS} \tag{2.1}$$

and taking into account the effects of $\boldsymbol{R}_S$ and $\boldsymbol{R}_D$, letting $V_{GS} = V_G$, the following quantity which does not depend on R_{SD} is obtained:

$$z = \frac{I_D^2}{I_D'} = \frac{K}{\gamma + 1} (V_G - V_T)^{\gamma+2} V_D \tag{2.2}$$

$$w = \frac{\int_{V_T}^{V_G} z dV_G'}{z} \cong \frac{\int_0^{V_G} z dV_G'}{z} = \frac{1}{\gamma + 3}(V_G - V_T) \tag{2.3}$$

The threshold voltage V_T, the mobility parameter K and the source-drain resistance R_{SD} can be extracted by using the quantities z and w [27].

V_T	γ	R_{SD}	**K**
-1.2 V	0.613	1.5 MΩ	$-8.76e-9$ F/Vs

Table 2.1. Parameter values obtained through used method.

The parameter values obtained by transfer curves have been employed in the compact model implemented in CAD environment. Simulated OTFT behaviours have been compared with experimental data as reported in Fig. 2.6.

2.5.2 AC parameters of OTFT compact model

Dedicated methods have been implemented to extract capacitance values through experimental data fitting. Fig. 2.7 represents experimental data of device impedance.

From the impedance analysis of experimental data different behaviours of gate-drain and gate-source impedances have been obtained. Moreover, a parametric study, using different impedance models (two RC parallel elements, three R series-RC parallel elements, four elements with Warburg impedance) has been carried out [28]. Results have been used to validate device impedance behavior with different polarization conditions. In particular, experimental conductance and capacitance mostly showed high variability respect to frequencies variations. Circuit analysis has been performed using the impedance frequency response characteristics in terms of both Bode and Nyquist analysis.

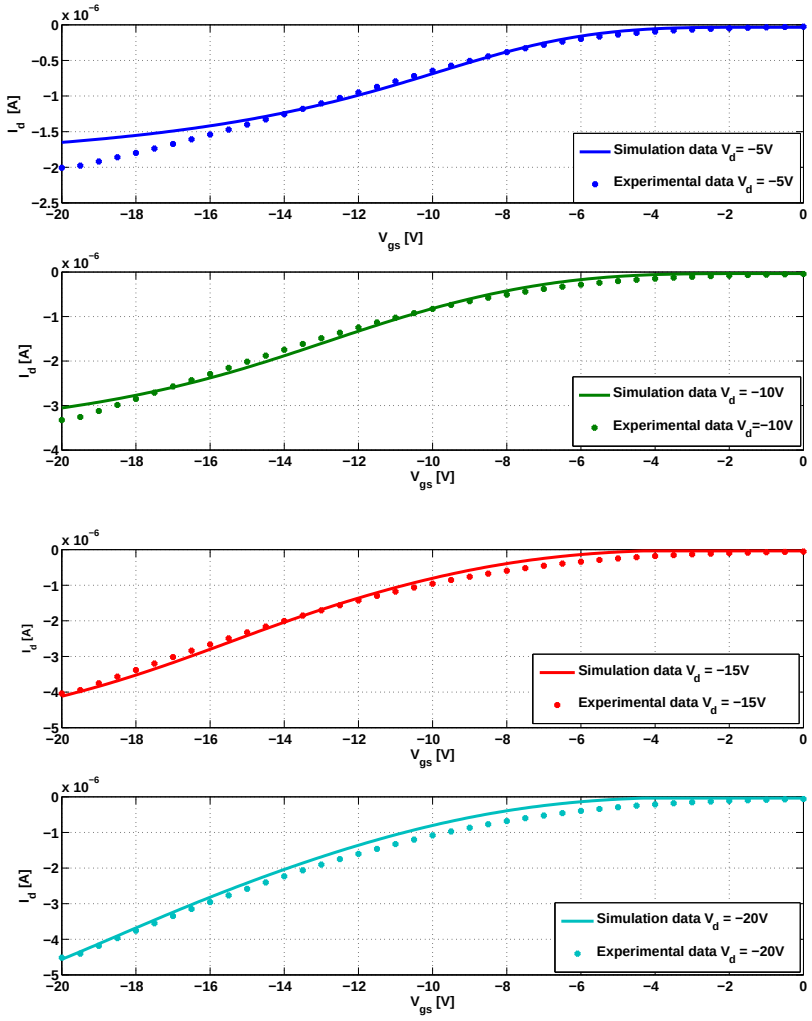

Fig. 2.6. Experimental and simulation data of OTFT. *Copyright [2009]EDP Sciences.*

Equivalent impedance model, with relative characteristic parameters, have been identified by fitting simulated Nyquist plot with experimental data (Fig. 2.8).

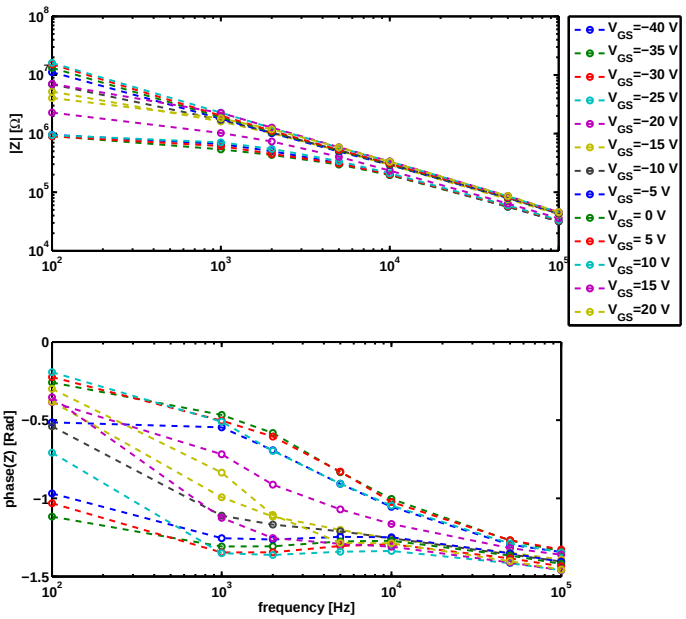

Fig. 2.7. Measurements of impedance phase and module. *Copyright [2009]EDP Sciences.*

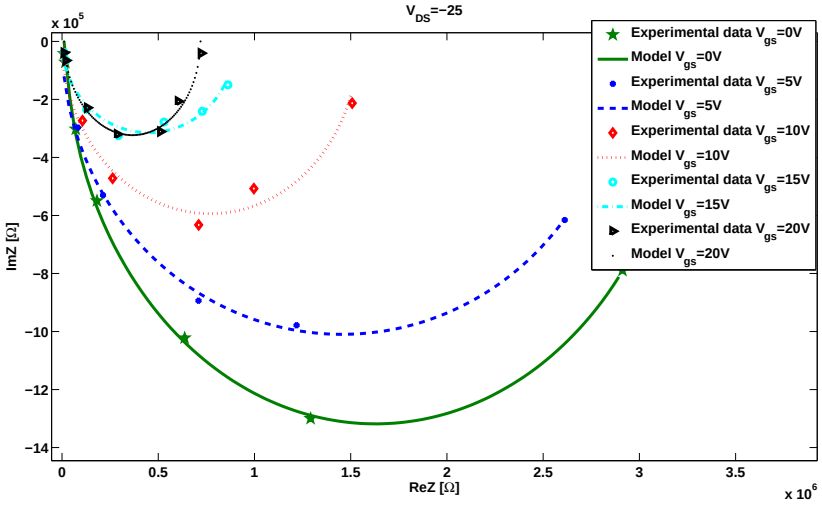

Fig. 2.8. Measured impedance and equivalent model fitting. *Copyright [2009]EDP Sciences.*

2.6 Considerations

The aim of this work was the development of a complete organic testing platform for organic device validation. A technology platform CAD flow has been defined to design organic circuits and layout, starting from OTFT model.

3

Organic Transducers Manufacturing using Different Solvents

The integration of IP^2C into all-organic electronic circuits have required a study about transducer performances. In this chapter an investigation of possible solvents for IP^2C membranes has been performed in order to increase their performances [29]. For the IPMC based actuators it is generally reported that solvents, different from water, can be used to avoid the dehydration phenomenon. In the same way, in this chapter the possibility to use Ethylene Glycol and an ionic liquid, 1-Ethyl-3 Methylimidazolium Trifluoromethanesulfonate, as diluents for IP^2C is investigated. Moreover, different materials have been used for device electrodes manufacturing and the performances of different organic transducers have been compared. Several devices have been realized and characterized by Scan Electrodes Microscopy (SEM) and Dynamic Mechanical Analysis (DMA). Their electromechanical behavior as actuators and sensors have been analyzed and a suitable material set has been identified.

3.1 Overview

All-organic electromechanical transducers, based on Nafion®117 as ionomer membrane, have been manufactured using different formulation of poly (3,4-ethylendioxythiophene)-poly (styrenesulfonate) (PEDOT:PSS) as electrode material.

If water is used as solvent for IP^{2}Cs they experience water loss that causes several limitations in term of performance and applications. In fact, the applied electric potential must be limited to less than 1.3V at room temperature, to avoid electrolysis and water evaporation in open air. Moreover, organic electrodes can degrade during sample hydration in the solvent. These problems can be overcome by using other than water solvents. E.g, Ethylene Glycol (EG) that, as water, consists of polar molecules, or 1-Ethyl-3 Methylimidazolium Trifluoromethanesulfonate (EmI-Tf), that is an ionic liquid existing as liquid at room temperature and shows high inherent stability [30] have been proposed for the case of IPMCs and will be taken into account here for IP^{2}Cs. Moreover, it is known that an enhancement in the conductivity can be obtained by adding to the conducting polymer different organic compounds (called secondary dopants or additives) such as several alcohol (diethylene glycol, 2-nitroethanol, glycerol) or high-boiling-point solvents (dimethyl sulfoxide, dimethylformamide, tetrahydrofurane). It is therefore possible to argue that to use EG and Ionic Liquids (ILs) in IP^{2}Cs, instead of water, can cause a beneficial effect on the electrical conductivity of PEDOT:PSS films. The conductivity enhancement is

strongly dependent on the changes of the chemical structure of the organic compounds, in particular on the conformational change that the secondary dopants determine into the polymer chains: the driving force is the interaction between the dipoles of the organic compound and dipoles or charges on the PEDOT chains [17]. Upon addition of EG or IL, conducting PEDOT:PSS grains merge together to form a three-dimensional conducting network [31], [32] determining an improvement of its electrical property. Moreover, an important difference between ILs and the high-boiling-point solvents, previously used as additives, is that ILs are not volatile and thus remains in the polymer conducting films. By substituting in the IP^{2}Cs the water with EG or an IL it is therefore possible to obtain both all-organic devices with low manufacturing cost, to overcome the dehydration problem and to improve electrical performance because of the enhancement of the electrical conductivity of PEDOT:PSS used as electrode. Different IP^{2}C prototypes have been manufactured and have been analyzed both morphologically through Scanning Electron Microscopy (SEM) and electrically, showing their electromechanical transduction behavior.

3.2 Manufacturing process

All-organic transducers have been realized based on a fluorocarbon membrane, Nafion® 117 (produced by Dupont®and distributed by Sigma-Aldrich Group, membrane thickness is 178 μm). The adhesion quality in thin film deposition strongly depends on surface properties;

for this reason, before the conductor deposition, Nafion® surface has been roughened. In order to remove water from the Nafion® membrane, it was dried at 100 °C for 24 hr, then it has been kept in vacuum for 3 hr.

3.2.1 Ethylene Glycol as solvent

In the first experiment, Ethylene Glycol (EG) was used as solvent for the Nafion® based IP^{2}Cs. Ethylene glycol viscosity is about 16 times higher than that of water at room temperature, and has a greater molecular weight. It is used as an anti-freezer. Like water, it consists of polar molecules and has been already suggested to be used as a solvent for IPMCs [33]. In Table 3.1 some chemical properties of EG are reported [34]. While Fig. 3.1 shows the chemical structure of EG [35].

Properties	
Relative Density	1.109 g/ml
Molecular weight	62.07 g/mol
Boiling Point	197.6 °C
Water solubility at 17.5 °C	10 g/100 ml
Melting point	-13 °C
Dielectric constant at 20 °C	41.4
Viscosity at 25 °C	$16.1 \cdot 10^{-3} Pa \cdot s$

Table 3.1. Some properties of ethylene glycol.

In order to obtain the IP^{2}Cs with EG as solvent, Nafion® membranes have been roughened and dried, soaked overnight in a beaker containing pure EG and, finally, heated to 60°C for 3 hr.

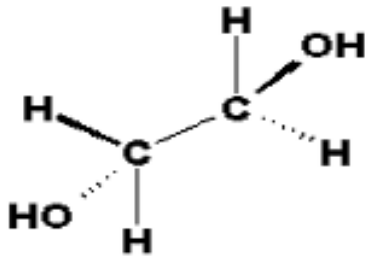

Fig. 3.1. Chemical structure of Ethylene Glycol.

3.2.2 Ionic liquid as solvent

In a second experiment, IP^{2}Cs using an ionic liquid as solvent have been produced. Ionic liquids are salts containing only charged species that exist in their liquid state at room temperature. They have an immeasurably low vapour pressure, electrochemical stability windows of 4 V or more, and are thermally stable to temperatures as high as 400°C. Furthermore, ionic liquids have high ionic conductivities and can be used as electrolytes for a variety of applications, including electrochemical capacitors [36] and conducting polymer actuators [37]. The ionic liquids are used as solvents for Nafion® based transducers for their stability and, therefore, to avoid the problem of solvent evaporation. Also, the ionic liquids are ionically conductive and should therefore facilitate ionic motion in the Nafion® membrane. In this work 1-ethyl-3 methylimidazolium trifluoromethanesulfonate (EmI-Tf) has been used: it has a viscosity of $35 \cdot 10^{-3}$ Pa· s - $45 \cdot 10^{-}3$ Pa· s at 25 °C. The more relevant properties of EmI-Tf are reported in Table 3.2 and in Fig. 3.2 its chemical structure is showed [38].

Properties	
Relative Density at 25°C	1.387 g/ml
Molecular weight	260.23 g/mol
Water solubility	fully soluble
Boiling Point	> 350 °C
Melting point	263-264 K (-9 °C)
Ionic conductivity	8.6-9.3 mS/cm
Electrochemical stability window	4.1 V

Table 3.2. Some properties of EmI-Tf.

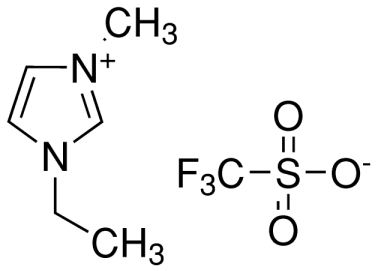

Fig. 3.2. Chemical structure of EmI-Tf.

To produce IP^{2}Cs with EmI-Tf as solvent, Nafion® membranes have been soaked, after roughing and drying, overnight in a beaker containing pure EmI-Tf and then heated to 140 °C for 3 hr.

3.2.3 Organic conductor

Poly (3,4-ethylendioxythiophene)-poly (styrenesulfonate) (PEDOT:PSS) is one of the best known conducting polymers: it shows excellent electrical conductivity as well as processability. E.g., for the case of Clevios^{TM} P HC V4 the conductivity value is 200 S/cm, as reported in [39]. In

this work, IP^{2}Cs have been fabricated using different formulations of PEDOT:PSS, reported in Table 3.3, to realize the electrodes.

Organic Conductor	Trade Name	Material Supplier
PEDOT:PSS	CLEVIOS^{TM} PH 500	H.C.Starck
	CLEVIOS^{TM} P HC V4	
	CLEVIOS^{TM} PH 510	
	Orgacon®EL-P 3040	AGFA

Table 3.3. Adopted conducting materials.

The conducting polymers have been applied on the Nafion® surface by drop-casting technique, since it is a very low cost procedure: the polymer has been spread over both sides of the Nafion® membranes (after they have been processed by using either EG or EmI-Tf, as described in the previous sub-sections). Eventually, IP^{2}Cs have been dried with an extractor fan and heated to 60 °C for 2 hr. Eight different IP^{2}Cs were produced and they are listed in Table 3.4 along with used sample codes.

Surface analysis of the samples has been performed by SEM in order to evaluate the layer adhesion and the film thickness. In Fig. 3.3 two SEM images of an IP^{2}C section are reported. More specially, these figures show a sample with Orgacon®EL-P 3040 electrode, whose thickness is about 6 μm - 7 μm, while the thickness of Nafion® 117 membrane is 178 μm. Fig. 3.3(a) shows tilted view and (b)-(c) report two

Organic material	Solvent	Sample code
CLEVIOS^{TM} PH 500	EG	EG-PH500
CLEVIOS^{TM} PH 500	EmI-Tf	EmI-PH500
CLEVIOS^{TM} P HC V4	EG	EG-PHCV4
CLEVIOS^{TM} P HC V4	EmI-Tf	EmI- PHCV4
CLEVIOS^{TM} PH 510	EG	EG-PH510
CLEVIOS^{TM} PH 510	EmI-Tf	EmI-PH510
ORGACON®EL-P 3040	EG	EG-3040
ORGACON®EL-P 3040	EmI-Tf	EmI-3040

Table 3.4. Samples manufactured and tested.

cross-section view of two samples. It is possible to observe that the PEDOT:PSS surface is highly inhomogeneous and rough.

3.3 Actuator electric characterization

Obtained IP^{2}Cs were cut into strips of size 2 cm x 0.5 cm and their electromechanical transduction capabilities were tested. More specifically, the free deflection produced was investigated. EmI-PH510 and EG-PH510 samples did not show good actuating performance, for this reason their characterization will not be reported in the following.

3.3.1 Actuator with EG as Solvent

A common set of experiments was defined for the IP^{2}C characterization and the evaluation of the suitable organic conductors to be used. A sinusoidal voltage signal with a frequency sweep from 50 mHz to 50 Hz

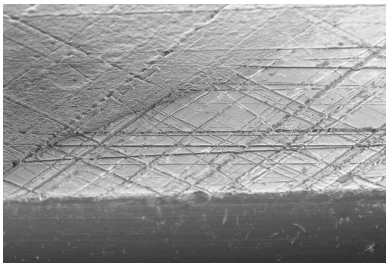

(a)

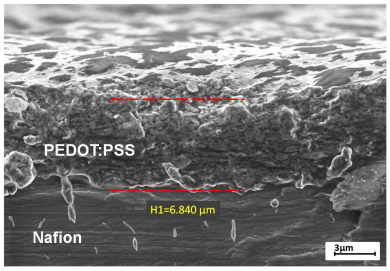

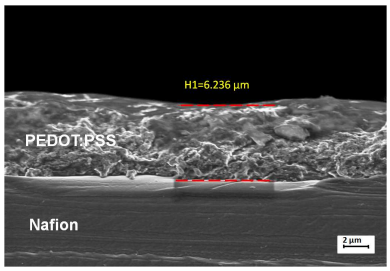

(b) (c)

Fig. 3.3. SEM images of an IP^{2}C tilted view (a)and cross sections(b)(c).

or 150 Hz and amplitude 3 V were applied to all samples and the corresponding absorbed current and sample displacement were measured and acquired. Data were used to estimate the IP^{2}C voltage to deformation transfer function of sample displacement and to evaluate sample's resonance frequency, in the hypothesis that a linear approximation for the IP^{2}C can be used.

Data recorded for EG-PH500, EG-PHCV4 and an EG-3040 are reported in Fig. 3.4. A perusal analysis of signals reported allows to conclude that the actuating behavior of the sample with Orgacon®EL-

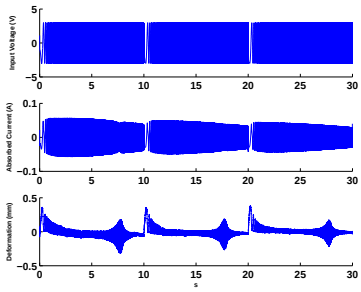

(a)

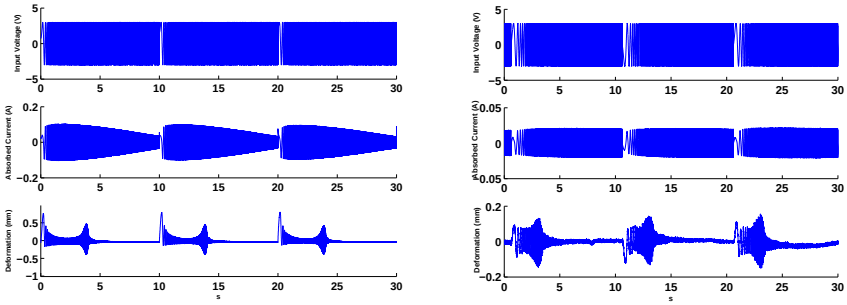

(b) (c)

Fig. 3.4. Actuator frequency sweep measurement with EG-PH500 (a), EG-PHCV4 (b) and EG-3040 (c).

P 3040 electrodes (EG-3040) is very poor, when compared with the behavior of other samples. It is, in fact, possible to observe that a very small and noisy deflection was obtained for the EG-3040 sample. As a further investigation, the magnitude of the voltage to deflection transfer functions for the same samples is seen in Fig. 3.5. For EG-PH500 the resonance frequency is about 76 Hz. This sample has the highest

resonance frequency, since the EG-PHCV4 sample resonance frequency is about 56 Hz, while EG-3040 resonance frequency is about 12 Hz.

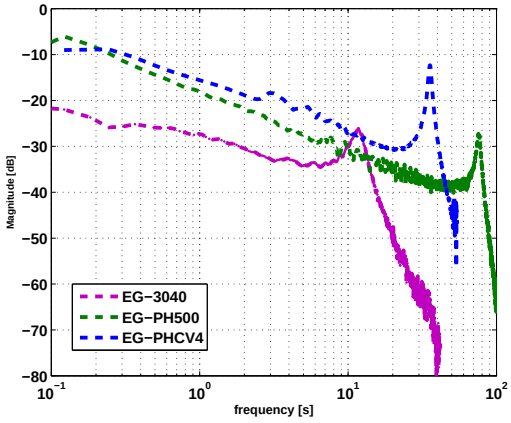

(a)

Fig. 3.5. Transfer function magnitude of EG-PHCV4(blue), EG-PH500(green)and EG-3040(magenta).

Sample	Resonance frequency	Absorbed Current	Deformation maximum
EG-PH500	76 Hz	0.06 A	0.4 mm
EG-PHCV4	56 Hz	0.1 A	0.8 mm
EG-3040	12 Hz	0.02 A	0.24 mm

Table 3.5. Obtained values of absorbed current, deformation and resonance frequency of IP^{2}Cs with EG.

Table 3.5 reports values of resonance frequency, absorbed current amplitude and maximum deformation values of the three tested IP^{2}Cs with EG.

3.3.2 Actuator with EmI-Tf as solvent

In a second set of experiments, the behavior of samples with EmI-Tf as solvent and with the organic conductors (see Table 3.4) were investigated, by using the same experimental conditions described in the previous sub-section: a swept voltage signal was applied to the samples EmI-PH500, EmI-PHCV4, and EmI-3040 and absorbed current and tip free deflection were recorded. Time records are shown in Fig. 3.6, while the corresponding transfer function magnitudes are reported in Fig. 3.7.

EmI-PHCV4 and EmI-PH500 have close resonance frequency and resonant peak amplitude values, whereas EmI-3040 shows both lower resonance frequency and resonant peak amplitude values.

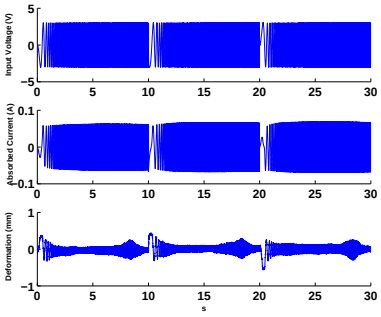

(a)

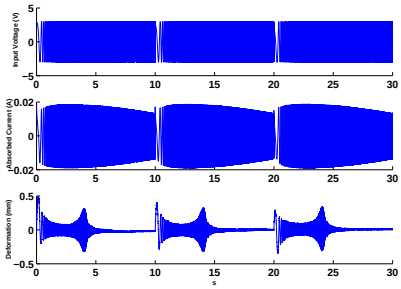

(b)

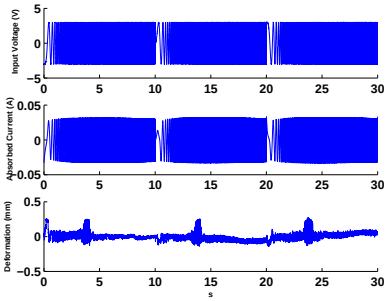

(c)

Fig. 3.6. Actuator frequency sweep measurement with EmI-PH500 (a), EmI-PHCV4 (b) and EmI-3040 (c).

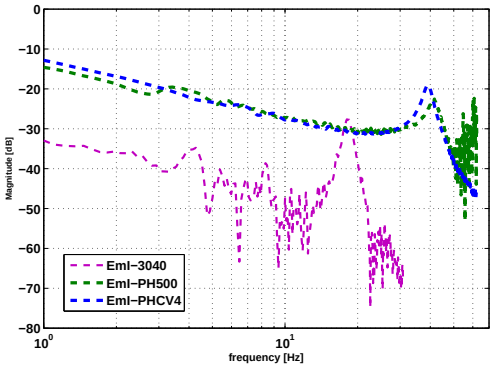

Fig. 3.7. Transfer function magnitude of EmI-PHCV4(blue), EmI-PH500(green)and EmI-3040(magenta).

Sample	Resonance frequency	Absorbed Current	Deformation maximum
EmI-PH500	41.6 Hz	0.06 A	0.4mm
EmI-PHCV4	39 Hz	0.02 A	0.7 mm
EmI-3040	18.4 Hz	0.031 A	0.27mm

Table 3.6. Obtained values of absorbed current, deformation and resonance frequency of IP^{2}Cs with EmI-Tf.

Table 3.6 reports values of the resonance frequency, absorbed current amplitude and maximum values of sample deformation obtained by tested IP^{2}Cs with EmI-Tf.

Results reported so far have shown that IP^{2}C that use Clevios^{TM} P HC V4 and $PH500$ gave best results in terms of applied voltage to produced deformation. Moreover, IP^{2}C based on PHCV4 showed better results in terms of stability. For such a reason in the following this last

class of devices will be in deeper analyzed to investigate the effects of EmI-Tf and EG on IP^{2}C behaviour.

3.3.3 Dynamic Mechanical Analysis (DMA)

DMA is a very versatile technique which can provide a convenient and sensitive testing system for rapid determination of thermo-mechanical properties of polymers and polymer-based materials as a function of frequency, temperature or time. The measurements were performed by means of Tritec 2000 DMA produced by Tritec: a sinusoidal tensile force was applied to the samples (in hydrated condition) in the range from 0.1 to 100Hz, at working temperature T=20 C. Measurements of the storage modulus and loss modulus (E' and E") as well as the damping parameter or loss factor ($tan\delta$), defined as the ratio $tan\delta$=E"/E', were obtained to compare the influence of the solvent in the mechanical properties IP^{2}Cs. It is important to take into account that elastic moduli measured by DMA often does not agree well with those obtained from mechanical testing methods [40]. In most cases, the elastic moduli measured by DMA are utilized only for screening material properties for the purposes of quality control, research and development of optimum processing conditions. Fig. 3.8(a) shows the DMA results for the storage modulus (E') of Nafion®, EG Nafion®, EG-PHCV4 as a function of frequency in tensile mode. Fig. 3.8(b) reports the results for the storage modulus (E') of samples with EmI-Tf. Fig. 3.9 shows the Loss moduli (E") of Nafion®, EG Nafion®, EG-PHCV4, EmI Nafion® and EmI-PHCV4 as a function of frequency in

tensile mode. Finally, Fig. 3.10 reports the $tan\delta$ of Nafion, EG Nafion, EG-PHCV4, EmI Nafion and EmI-PHCV4.

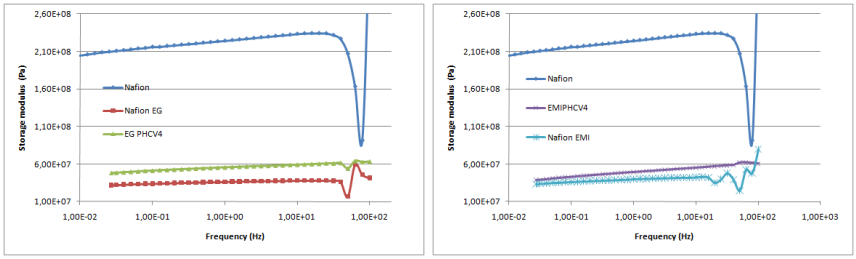

(a) (b)

Fig. 3.8. Storage modulus (E') of Nafion, EG Nafion and EG-PHCV4 Nafion (a); EmI Nafion and EmI-PHCV4(b) as a function of frequency.

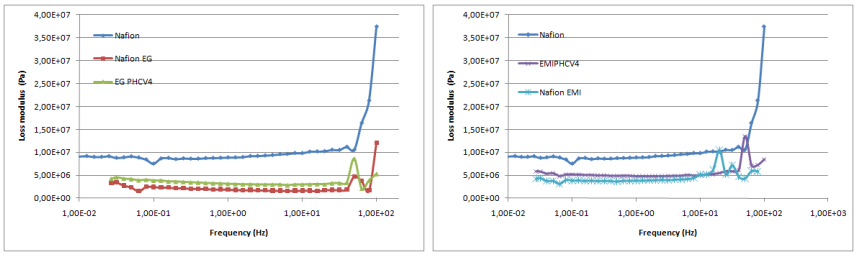

(a) (b)

Fig. 3.9. Loss modulus (E") of Nafion, EG Nafion and EG-PHCV4 Nafion (a); Nafion, EmI Nafion and EmI-PHCV4(b) as a function of frequency.

By comparing the data relative to Nafion® with those of the other samples, it is evident that the presence of the solvent has a plasticizer effect leading to the reduction of the tensile strength by disconnecting

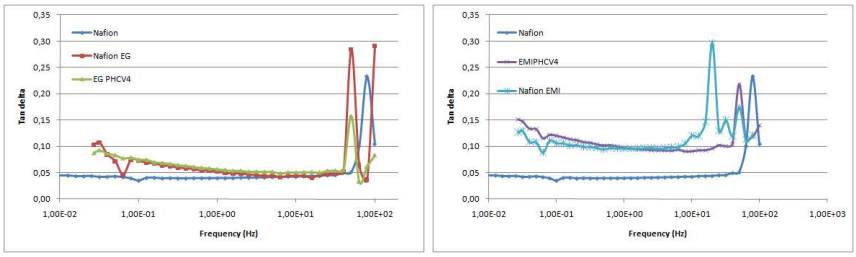

(a) (b)

Fig. 3.10. *tanδ* of Nafion, EG Nafion and EG-PHCV4 Nafion (a); Nafion, EmI Nafion and EmI-PHCV4 as a function of frequency.

the membrane polymer chains and determining a volume change of base materials. The presence of the electrode (conducting polymer) determines an increase in the modulus value.

3.3.4 Electromechanical transduction

In this section, the two IP^{2}C considered in the previous subsection are investigated with respect to their electromechanical transduction. The frequency behaviour of IP^{2}Cs has been tested by using a set of three consecutive swept signals. The magnitudes of the transfer functions of the two samples are shown in Fig. 3.11(a) and (b), respectively. Experiments have shown that, at least for very short repetition times of the experiments, the frequency response of the devices are quite close one each other. More specifically a good agreement has been obtained for the values of their resonance frequency.

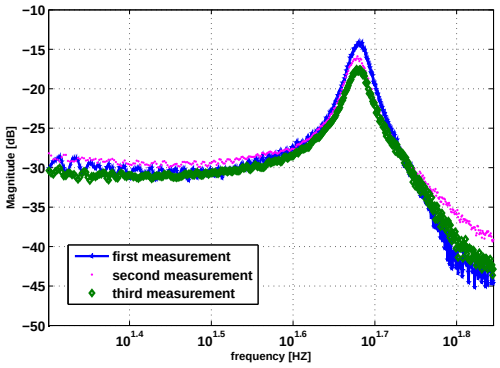

(a)

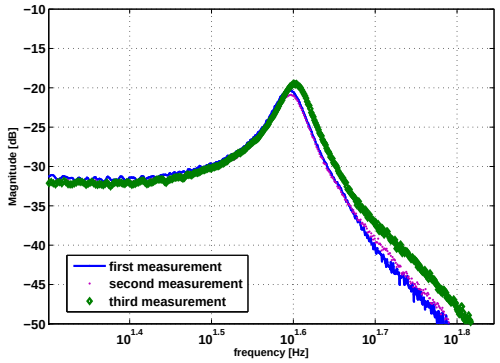

(b)

Fig. 3.11. Consecutive measurements of a EG-PHCV4 sample (a) and a EmI-PHCV4 sample (b).

The transfer function magnitudes of the two samples are compared in Fig. 3.12. The EmI-Tf sample displays a lower magnitude than the sample with EG. Also resonance frequency obtained with EG is higher.

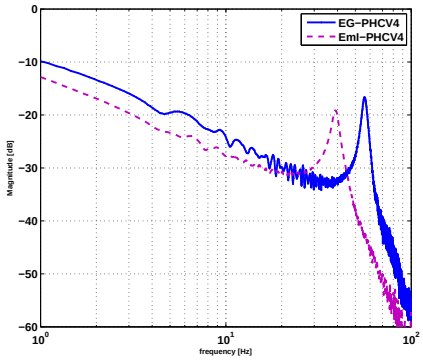

Fig. 3.12. The magnitudes of the transfer functions of EG-PHCV4 and EmI-PHCV4 samples.

3.4 Sensor electric characterization

Sensor behaviour has been tested for all kinds manufactured membranes with different electrodes and solvents discussed previously. Moreover, also deionized water has been used for transducers and investigated in this section. The sensor has not problem of water hydrolysis and, therefore, the membranes did not need to be rehydrated. Moreover, IP^{2}C sensor works in good condition when the sample is not very hydrated. For this reason, samples with water as solvent have been characterized and their sensing currents have been reported.

The experimental setup of Fig. 1.4(a) has been used in order to detect the performances of polymeric sensors. The Fig. 3.13 shows sensing currents produced by samples with deionized water applying periodic impulsive impacts. The interesting result is that the sample with ORGACON® EL-P 3040 shows the best result in term of sensing current than other samples. As it will be shown in following results only in this case ORGACON® EL-P 3040 allows to IP^{2}C to produce higher current than other organic conductors.

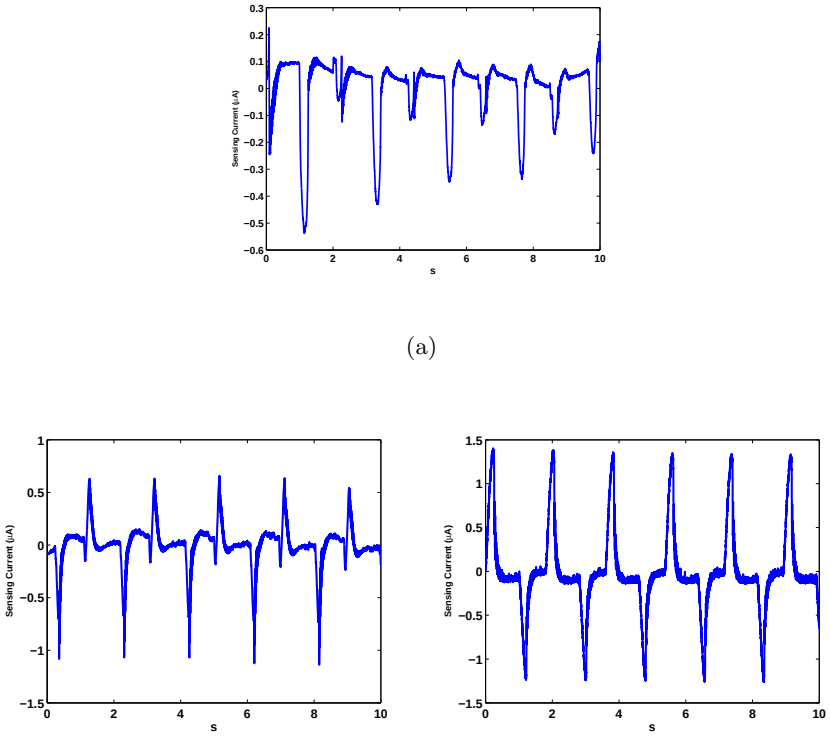

(a)

(b) (c)

Fig. 3.13. Sensor measurement with H2O-PH500 (a), H2O-PHCV4 (b) and H2O-3040 (c).

The Fig. 3.14 show sensing currents produced by EG-PHCV4, EG-PH500 and EG-3040 samples applying periodic impulsive impacts.

Fig. 3.15 show sensing currents produced by EmI-PHCV4 , EmI-PH500 and EmI-3040 samples applying periodic impulsive impacts.

These sensor measurements allow to detect the devices that produce the larger sensing current for the same applied deformation. In detail, the sample with ORGACON® EL-P 3040 electrodes generates

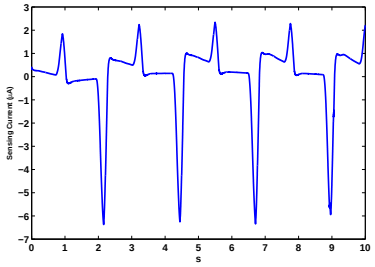

(a)

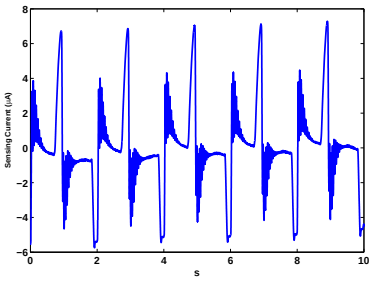

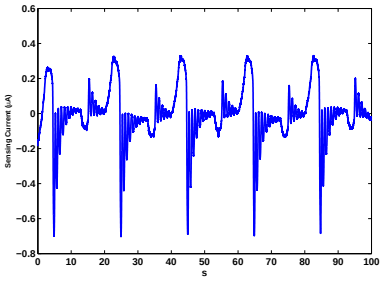

(b) (c)

Fig. 3.14. Sensor measurement with EG-PH500 (a), EG-PHCV4 (b) and EG-3040 (c).

a smaller current than other devices both with EG and EmI-Tf. Moreover, from the graphs of the sensing currents it is possible to notice that the EG solvent produced samples with better performances than EmI-Tf membranes. These analyses are determinant in order to identify the organic conductor for electrodes and the solvent to be used to obtain good sensing performances.

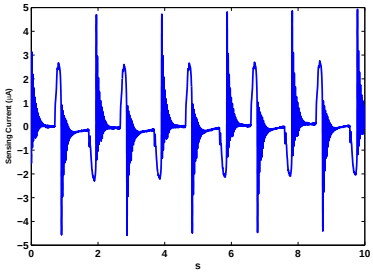

(a)

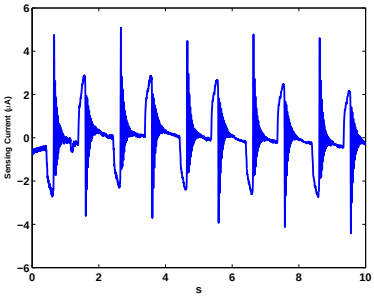

(b)

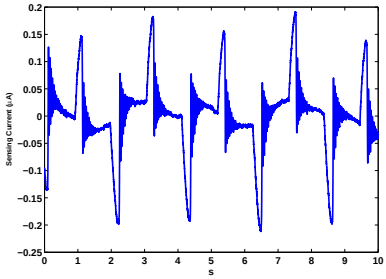

(c)

Fig. 3.15. Sensor measurement with EmI-PH500 (a), EmI-PHCV4 (b) and EmI-3040 (c).

3.4.1 Equivalent circuit of IP^{2}C sensor modeling

In order to develop novel smart applications the electromechanical transducers have been characterized and its behavior has been modeled. The polymeric composite sensing device has been modeled by defining the dynamical system that transforms the applied mechanical stimulus into the sensor electric reaction. The IP^{2}C membranes demonstrated sensor capabilities to detect mechanical deformation. An IP^{2}C sensor device structure is shown in Fig. 3.16, where $f(t)$ is the applied force, $\delta(t)$ is the deflection of the beam and $I_S(t)$ obtained in short-circuit condition.

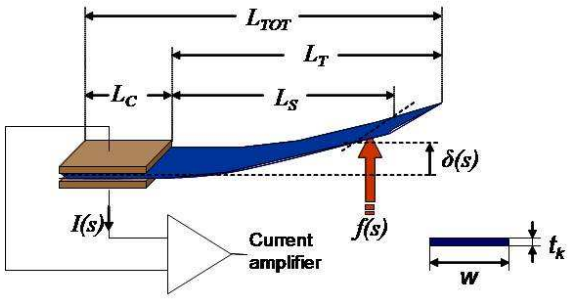

Fig. 3.16. Parameters characterizing the actuator and sensor devices

An electric equivalent circuit has been obtained starting from the electromechanical model [41] of the IP^{2}C sensor described by Equation 3.1.

$$I(s) = k\frac{3t_k wY}{4L_s} \cdot \frac{s}{(s+a)}\delta(s) \tag{3.1}$$

The circuit, shown in Fig. 3.17, comprises an RC structure, introduced to model the intrinsic capacitive nature of the membrane.

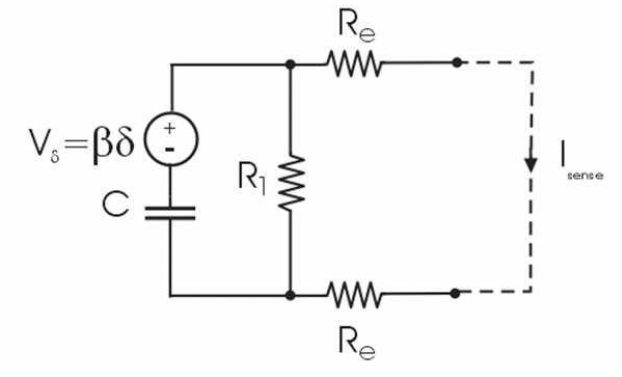

Fig. 3.17. Electric equivalent circuit of IP_2C sensor model.

Two resistances R_e has been introduced in order to model the organic conductor resistive effect. Moreover the resistance R_1 has been introduced to model the equivalent bulk resistance of Nafion® in DC conditions. In order to parameterize the model as a function of membrane dimensions the resistance R_1 is expressed in terms of the Nafion®DC resistivity ρ_1 and the geometrical parameters as defined by Equation 3.2.

$$R_1 = \frac{\rho_1 \cdot t_k}{L_{TOT} \cdot w} \tag{3.2}$$

The value of ρ_1 in agreement to Dupont datasheets is 1205Ωm. The capacitors C has been expressed in terms of the permittivity ε and membrane geometric quantities according to the relation 3.3.

$$C = \varepsilon \cdot \frac{L_{TOT} \cdot w}{t_k} \tag{3.3}$$

The organic electrodes resistance R_e is also expressed by Equation 3.4 as a function of the membrane dimensions and suitable parameter R_S

$$R_e = R_S \cdot \frac{L_T}{w} \tag{3.4}$$

The value of R_S has been obtained from the identification procedure reported in [9]. The electromechanical transduction has been modeled by means of the voltage source generator V_δ controlled by the displacement $\delta(t)$. The term β is a proportionality coefficient which models the coupling between the input displacement and the voltage applied to capacitor C. The relations which associate the electric circuit parameters ε and β to the electromechanical model parameters of Table 3.4.1 are expressed by Equation 3.5 and Equation 3.6 where R_P is the equivalent parallel resistance between R_1 and $2R_e$.

$$\varepsilon = \frac{t_k}{L_{TOT} \cdot w \alpha R_P} \tag{3.5}$$

$$\beta = \frac{3}{2} t_k Y k R_S \tag{3.6}$$

Y	**k**	α
$4.6027(GPa)$	$2.1373 \cdot 10^{-8}(CsN^{-1})$	$-13.0838(Hz)$

Table 3.7. Sensor model identified parameters.

The obtained normalized circuit parameter values are reported in the Table 3.4.1.

R_S	β	ε
$52.5806(\Omega m/m)$	$1.5514(V/m)$	$6.226 \cdot 10^{-4}(F/m)$

Table 3.8. Equivalent circuit parameters.

The sensor model, reported in [9], has been described in order to explain its implementation in CADENCE® environment, reported in Chapter 5.

3.5 Considerations

In this chapter the electromechanical transduction properties of different IP^{2}Cs have been compared. Samples have been manufactured by using several conducting polymers and different solvents. More specifically, solvents, different from pure water, have been taken into account in order to overcome its limits: the used solvents allow to use higher voltage values and to avoid the hydration phase that is incompatible with some organic conductors. The IP^{2}C shows better performances with Clevios^{TM} P HC V4 and with Clevios^{TM} PH 500 both during actuator and sensor characterization. Moreover, both solvents allow transducers to obtain considerable actuating behavior, but better features have been observed with EG than EmI-Tf. In case of sensor behaviour EG solvent allows to obtain higher values of current.

4

New Techniques for Electrodes Deposition

The research activity on polymeric transducers was focused on increasing their performance overcoming the limits of samples hydration. New manufacturing techniques have been taken in account in order to allow soaking in solvents. In this chapter, other methods for electrodes manufacturing have been investigated to permit the rehydration after actuator or sensor electromechanical functioning. Moreover, these techniques have permitted to use water as solvent in devices with conductors that solve in water.

4.1 Organic electrodes manufacturing

In previous chapters the adhesion problem of polymer conductor was discussed. In fact, the Nafion® sample was processed through the sandblasting in order to limit the problem. This processing consists in membrane roughening where organic conductor was deposed by drop casting technique. In Fig. 4.1 two SEM images are reported showing

that conductor layer is not totally adhered to Nafion®membrane. Moreover, during hydration phase, when samples are soaked in solvent, after few seconds, the conductor layers peel off Nafion®. When water is employed as solvent for actuator IP^2C the rehydration destroys the sample.

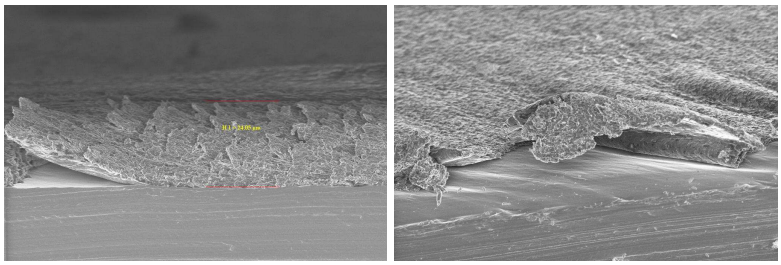

(a) (b)

Fig. 4.1. SEM images where organic electrode is teared out from Nafion membrane.

For these reasons other techniques for Nafion® processing and for organic conductor deposition have been analyzed and employed.

4.1.1 Chemical roughening

This technique allows to increase the quality of adhesion of organic conductor with Nafion® membranes. It is based on chemical roughening by treatment with sulfuric acid (H_2SO_4) and hydrogen peroxide (H_2O_2). The chemical roughening consists in boiling Nafion® membranes in a solution of sulfuric acid, H_2SO_4 1M (under stirring) for a half hour, then in H_2O for half an hour. Successively, the membrane is boiled in

hydrogen peroxide, H_2O_2 3%, and again in H_2O. Also these last treatments are kept for a half hour. This treatment leaves Nafion® surfaces more inclined to adhere with organic conductor.

After this preliminary treatment the organic conductor is deposited through drop casting or with another technique that polymerizes the conductor directly on Nafion® membrane. In the first case, the results have been not satisfactory, due to the fact that the electrodes deposed through drop casting techniques, are degraded and separated by Nafion®membrane during hydration phase. In the second case, membranes soaking inside solvent is successful.

4.1.2 Electrodes polymerization on Nafion® membranes

In a typical film deposition experiment [42], EDOT (0.426 g, 3 mmol), NaPSS (0.1236 g, 0.6 mmol) and H_2O (160 ml) were stirred at 50 °C until a clear solution was obtained. The solution was allowed to cool to room temperature and pieces of Nafion® 117 membranes were then soaked. Solid $Fe(NO_3)_3 9H_2O$ (3.303 g, 7.5 mmol) was then added. The solution was stirred for 1 hr. This resulted in a dark blueblack PEDOT layer being deposited on both sides of the membrane pieces. The membranes were then removed from the polymerization solution and well rinsed with distilled water. Then the samples were boiled in H_2SO_4 1 M for 1 hr in order to perform the exchanging of Fe^{3+} with H^+ ions, then they were boiled in distilled H_2O for 1 hr and stored in distilled water.

Fig. 4.2. Hot plate/stirrer used for chemical roughening and polymerization.

Three samples have been prepared with different time of polymerization: one hour, half an hour and a quarter of an hour. Polymerization time is an important factor during electrodes manufacturing, in fact this determines the thickness of the conducting layer. Consequently, it can change both device stiffness and electrode conductivity, two main features for IP^{2}Cs. The prepared membranes are IP^{2}Cs with water inside as solvent. Other samples are prepared in same way, but H_2O inside membranes was substituted with Ethylene Glycol(EG).
They present uniform surfaces due to the fact that the distribution of conductor is underlined by the uniform color (dark blue) of the electrode, as reported in Fig. 4.3.

4.2 Electromechanical characterization

The samples have been tested through the experimental setups described in Chapter 1, in order to compare and analyze the device performances both as actuator and sensor. In detail, six different IP^{2}Cs

Fig. 4.3. Membrane of IP^{2}C realized through electrodes polymerization.

have been produced with chemical roughing and EDOT polymerization on Nafion® and they are listed in Table 4.1 along with used sample codes.

Polymerization time	**Solvent**	**Sample code**
1 hour	EG	$1h\_EG$
1 hour	H_2O	$1h\_H_2O$
half an hour	EG	$1/2h\_EG$
half an hour	H_2O	$1/2h\_H_2O$
quarter an hour	EG	$1/4h\_EG$
quarter an hour	H_2O	$1/4h\_H_2O$

Table 4.1. Samples manufactured and tested.

Other two samples have been produced by using the chemical roughing and drop casting technique for electrodes manufacturing. PEDOT deposed on Nafion® membrane is Clevios^{TM} P HC V4, which has been discussed previously. Ethylene glycol allows to avoid rehydration phase and thus sample with EG can be tested to obtain their complete characterization, while sample with water can not be retested after a

first measurement set, because dehydrated. The used codes to identify these samples are $RoughPHCV4EG$ and $RoughPHCV4H_2O$.

4.2.1 Actuator behaviour

In this section different polymerization times are compared. Moreover, the solvents effect in these new samples have been observed. A swept signal of amplitude 3 V and a growing frequency (from 0.1 Hz to 100 Hz) has been applied to samples through the measurement setup. Fig. 4.4 shows the comparison between two samples with H_2O as solvent and different polymerization times: one hour and a quarter an hour, respectively. The behaviour of $1h\_H_2O$ is reported in blue color while $1/4h\_H_2O$ behaviour is shown in green color. The first shows a higher deformation with a consequent higher absorbed current then the second sample. Moreover, water inside membranes evaporates during measurement generating a decreasing trend of deformation as it is more visible for the fist sample. Fig. 4.4(b) shows the bode diagram for the two samples from which resonance frequency can be evaluated. The $1/4h\_H_2O$ sample presented a higher resonance frequency than $1h\_H_2O$.

A similar comparison has been performed with EG solvent. In detail, two samples with different polymerization time have been tested and compared: $1h\_EG$ (light blue) and $1/2h\_EG$ (magenta). Fig. 4.5(a) shows sample responses to the swept signal. They have a similar response in term of deformation, while absorbed currents are very different. In fact, the sample $1h\_EG$ absorbs less current than $1/2h\_EG$.

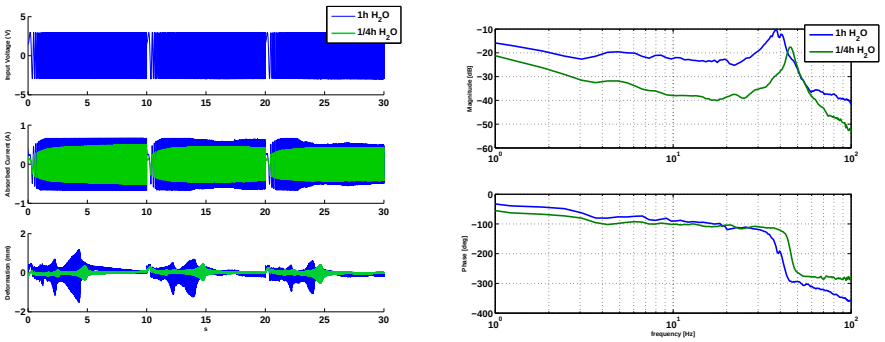

(a) (b)

Fig. 4.4. Actuator frequency sweep measurement with $1h\_H_2O$ (blue) and $1/4h\_H_2O$(green): output signal (a), bode diagram (b).

Bode diagram, showing the response in frequency in term of deformation, presents a similar behaviour of both samples.

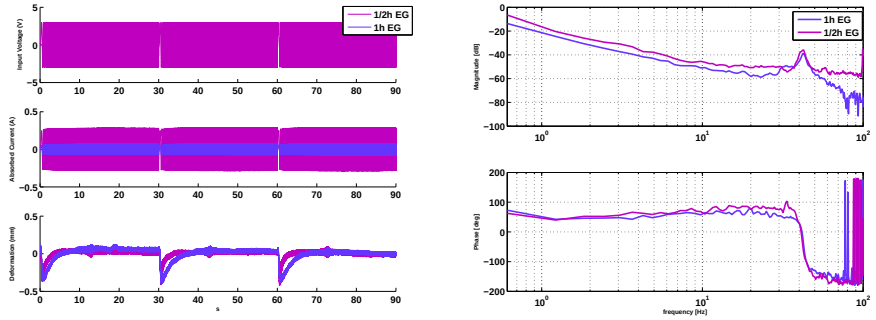

(a) (b)

Fig. 4.5. Actuator frequency sweep measurement with $1h\_EG$ (light blue) and $1/2h\_EG$(magenta): output signal (a) and Bode diagram (b).

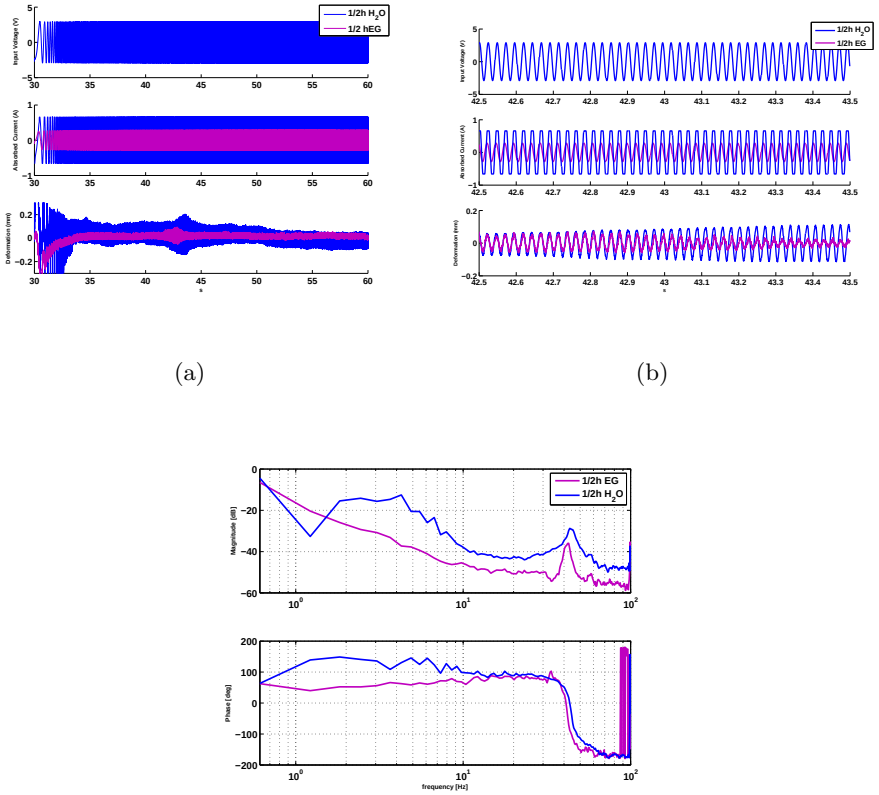

(a) (b)

(c)

Fig. 4.6. Actuator frequency sweep measurement with $1/2h\_EG$ (magenta) and $1/2h\_H_2O$(blue): output signal (a), a zoom (b) and Bode diagram (c).

Finally, the solvent effects inside same type of IP^{2}C have been investigated. In detail, same polymerization time has been taken in account: half an hour. Fig. 4.6 reports a sweep period of responses of $1/2h\_EG$ (magenta) and $1/2h\_H_2O$(blue) in order to compare their behaviours with H_2O and EG. Although the water presents several limitations dur-

ing actuator functioning, it shows a better actuating behaviour than EG. Moreover, Fig. 4.4,4.5 and 4.6 underline that water performs better than the other solvent.
The high molecular weight of EG and high stiffness due to polymerization time decrease actuation performances.

Moreover, the $RoughPHCV4EG$ sample has been tested several times thanks to solvent type, on the other hand, the $RoughPHCV4H2O$ has been actuated only one time because the conductor layers peel off from Nafion® during hydration.

The Fig. 4.7 shows the results obtained by actuation of membrane $RoughPHCV4EG$: output signals applying a sweep of frequency and the bode diagram of obtained deformation.

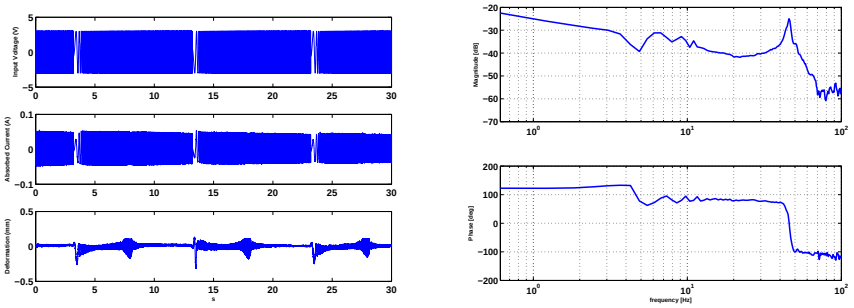

(a) (b)

Fig. 4.7. Actuator frequency sweep measurement with $RoughPHCV4EG$ sample: output signal (a) and (b) Bode diagram.

The Fig.4.7 shows the results obtained by actuation of membrane $RoughPHCV4H_2O$.

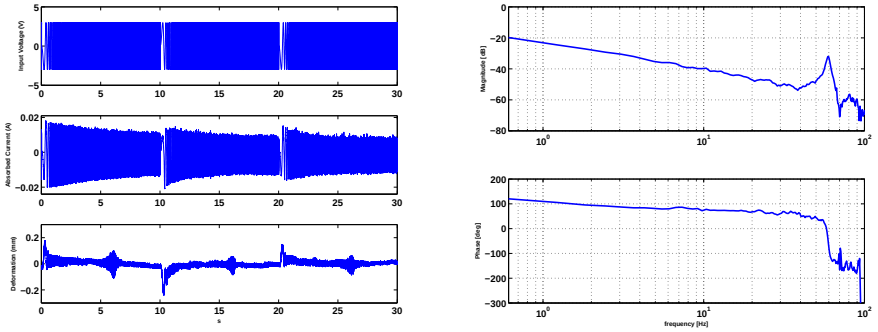

(a) (b)

Fig. 4.8. Actuator frequency sweep measurement with $RoughPHCV4H_2O$ sample: output signal (a) and bode diagram (b).

$RoughPHCV4H_2O$ is characterized by a higher resonance frequency although deformation amplitude is lower than $RoughPHCV4EG$.

Starting from these first analyses it has been deduced that water is an excellent solvent permitting a good actuator behaviour. This result is confirmed for sample realized with EDOT directly polymerized on Nafion®. Instead, when drop casting techniques is used to manufacture electrodes, EG solvent causes a beneficial effect on the electrical conductivity of PEDOT:PSS films allowing an improvement of device performances.

4.2.2 Sensor behaviour

Sensor behavior has been electrically investigated in several samples of Table 4.1. Two signals have been used and applied to the vibration system (TIRA Schwingtechnik TV50009), described in Chapter 1, for analyzing samples performances. A sweep voltage signal with a frequency range from 5 Hz to 150 Hz and peak to peak amplitude of 3 V has been applied. Moreover, it has been also used a white noise with maximum amplitude 1.5 V and in the same frequency range in order to further investigate the sensor behaviour. The effective applied tip displacement has been measured by means of a laser proximity sensor. The sensing current produced by the sample has been acquired through a conditioning circuit and a DAQ card. Some interesting measurements have been reported in this section. The sample $1h\_H_2O$ has been tested with the swept signal. Fig. 4.9(a) and (b) repots a measurement period and a zoom, respectively.

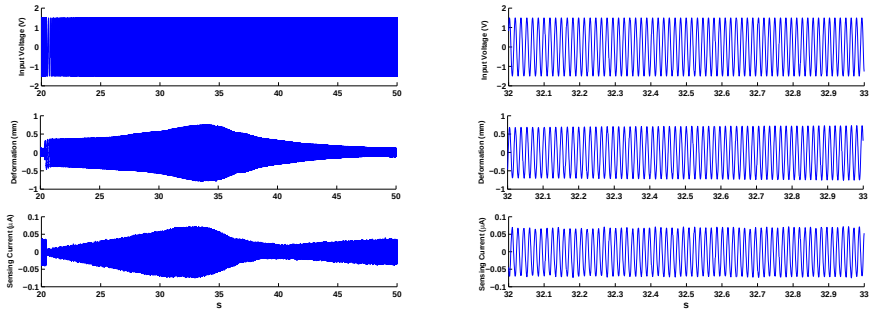

(a) (b)

Fig. 4.9. Actuator frequency sweep measurement with $1h\_H_2O$ sample: a measurement period (a) and a zoom(b)

The Bode diagram and the coherence function have been estimated from available data and are shown in Fig. 4.13(a) and (b), respectively. The coherence function measures the correlation between applied deformation(x) and sensing current(y) at each frequency value. The magnitude squared coherence estimate is a function of frequency with values between 0 and 1 that indicates the correspondence in frequency between two signals.

Also noise signal has been applied to the samples. The results are reported in Fig. 4.11. The Bode diagram confirms the frequency behaviour obtained by the sweep measurement, previously reported.

Considering the same polymerization time the sample with EG has been tested applying the swept signal in order to analyze solvent effects. Fig. 4.12 shows a measurement period (a) and a zoom in order to

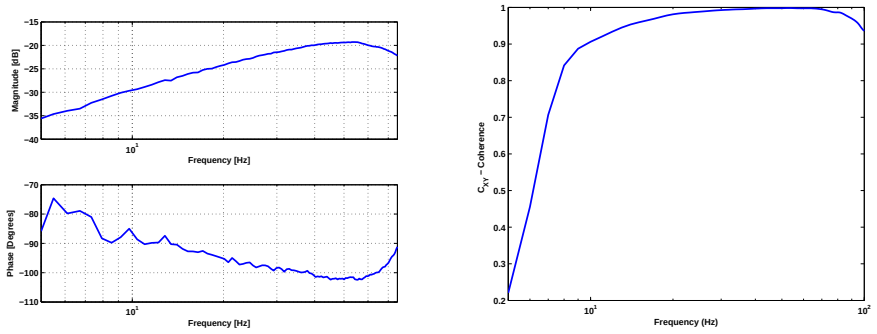

(a) (b)

Fig. 4.10. Bode diagram (b) and coherence function deformation-sensing current (c) of $1h\_H_2O$ sample.

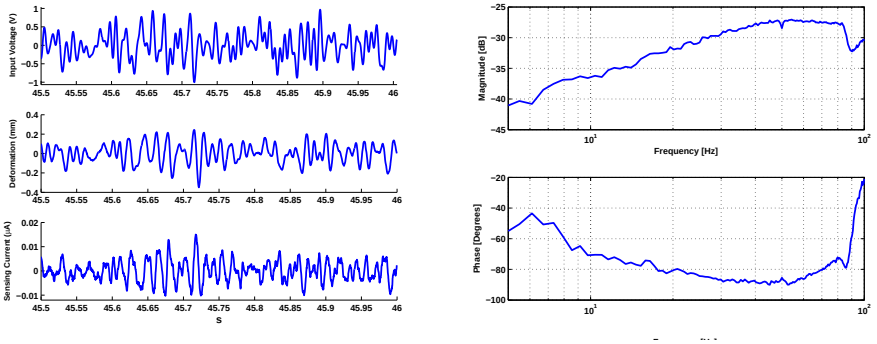

(a) (b)

Fig. 4.11. Actuator noise measurement with $1h\_H_2O$ sample: a zoom of measurement (a) and bode diagram (b).

observe the trend of signals. Comparing two samples with different

solvents, it is deduced that water allows to the membrane to produce higher current than EG.

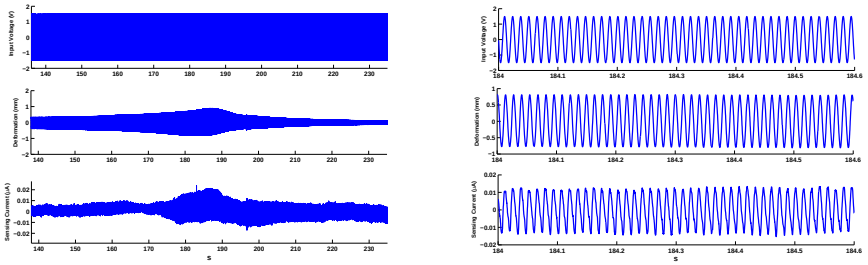

(a) (b)

Fig. 4.12. Actuator frequency sweep measurement with $1h\_EG$ sample: a measurement period (a) and a zoom(b).

Moreover, the graphs of Fig. 4.13 show that the used frequency range is too large. In fact, the coherence function shows its maximum value up to 50 Hz. For this reason the measurement has been repeated applying a swept signal, with a smaller frequency range, as shown Fig. 4.14 and Fig. 4.15.

Fig. 4.16 and Fig. 4.17 report measurement results obtained by $1/2\_H_20$ and $1/4\_H_20$ samples, tested by using a sweep signal. The $1/2h\_H_2O$ and $1/4h\_H_2O$ samples have been analyzed in order to compare the effect of polymerization time in IP^{2}C manufacturing. Both the samples have produced higher sensing current than $1h\_H_2O$. In fact, both samples with shorter polymerization time have generated a

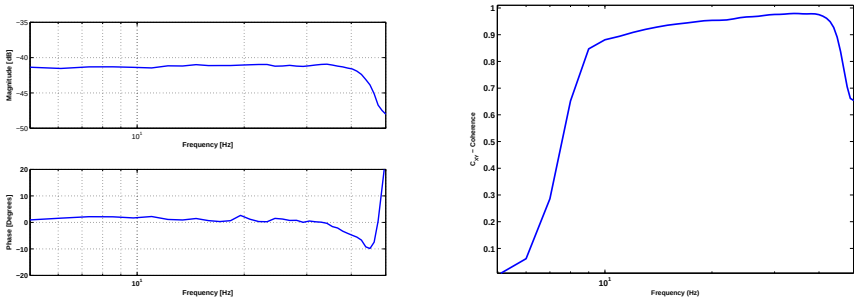

(a) (b)

Fig. 4.13. Bode diagram (b) and coherence function deformation-sensing current (c) of $1h\_EG$ sample.

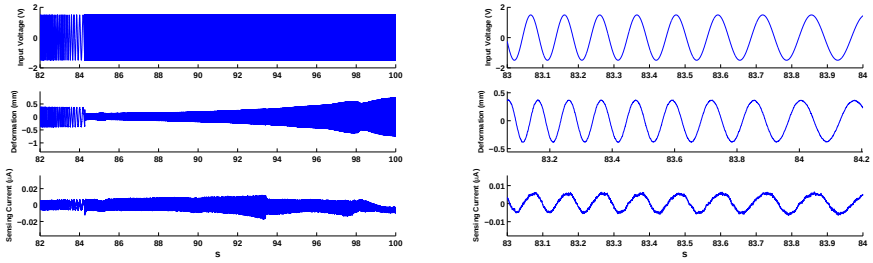

(a) (b)

Fig. 4.14. Actuator frequency sweep measurement with $1h\_EG$ sample: a measurement period (a) and a zoom (b).

sensing current of amplitude about 0.5μA while $1h\_H_2O$ sample has produced 0.05μA.

Therefore, observing the figures it is deduced that sensing current increases with decreasing of polymerization time.

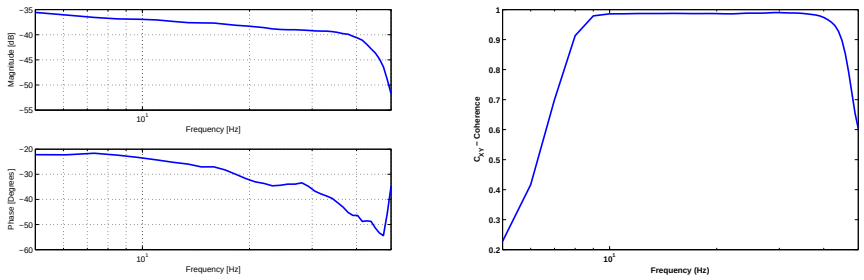

(a) (b)

Fig. 4.15. Bode diagram (b) and coherence function deformation-sensing current (c) of $1h\_EG$ sample.

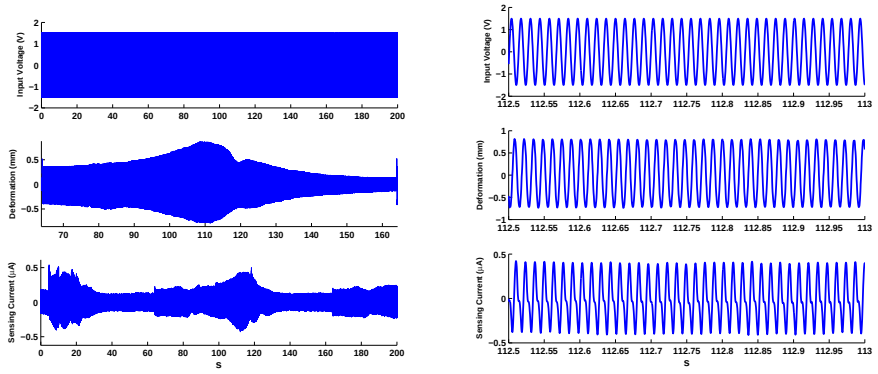

(a) (b)

Fig. 4.16. Actuator frequency sweep measurement with $1/2\_H_20$ sample: time sweep (a) and a zoom (b).

4.3 Considerations

The IP^{2}Cs have been manufactured through EDOT polymerization directly on Nafion® membrane and their electromechanical proprieties

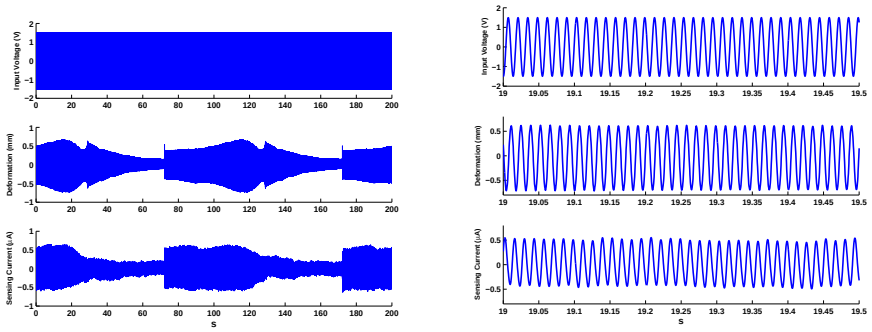

(a) (b)

Fig. 4.17. Actuator frequency sweep measurement with $1/4\_H_20$ sample: time sweep(a) and a zoom (b).

have been observed both with water and EG solvent. In particular, the water samples have shown a good behaviour both during sensor and actuator characterization. The higher molecular weight of EG is a fundamental factor that limits actuator deformation and sensor current. While, the polymerization time have produced different results in two cases. Organic transducer with electrodes polymerized for one hour have produced better performances both in term of absorbed current and deformation. Instead, current sensor grows with decreasing of polymerization time, in fact, the $1/2\_H_20$ and $1/4\_H_20$ samples have produced a higher current for same applied displacements.

5

All-Organic Embedded System Design

Organic electronics and polymeric transducers have been combined in order to design an embedded system with innovative materials. A model has been implemented in CADENCE® environment to design a system that includes both the IP^{2}C sensor model and the organic peak detector schematic able to sense the deformation of the system. The entire circuit has been simulated by means of Mentor Graphics ELDO in CADENCE® environment. Moreover, the device layout has been realized by using Virtuoso® Layout Editor for possible device manufacturing. This activity has been developed in STMicroelectonics Labs.

5.1 OTFT model implemented in CAD environment

The organic electronics research activity has been focused on p-type transistors by considering dedicated architectural solutions like ratioed

logic p-type circuitries. Organic devices are composed by layers of organic conductor, semiconductor or insulator as depicted in Fig. 5.1 where a transistor with top-gate and bottom-contacts configuration is shown. Organic thin-film transistors are field-effect devices with organic thin-film semiconductors as active layer. In terms of performance, or-

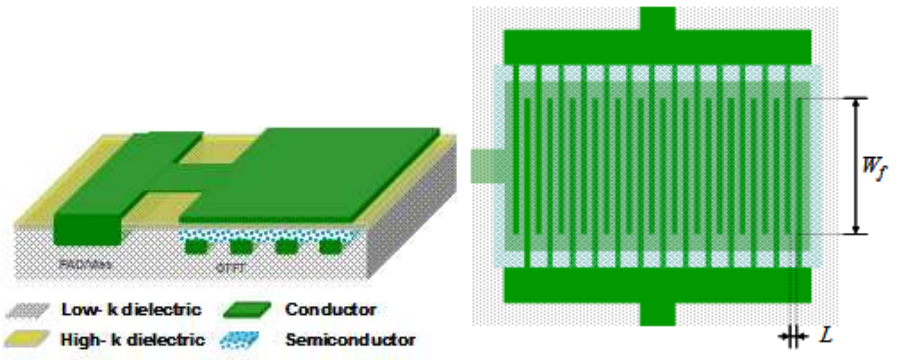

(a) (b)

Fig. 5.1. (Schematic 3-D view of an interdigitated OTFT with a gate pad (a) and multifinger structure (b).

ganic transistors cannot be compared to inorganic semiconductor based transistors, however, the opportunity to realize low cost, large area, and flexible devices, by using low-cost manufacturing techniques, can open the way to the development of new electronic applications [43]. To date, several studies have also been performed on n-type organic transistors but these transistors still remain not stable and feasible, unlike its p-type counterpart. Thus, the printed electronics research activity has been focused on p-type transistors by considering dedicated architec-

tural solutions. The adopted OTFT has a top-gate architecture with a conduction channel between the drain and source contacts characterized by the width W and the length L tuning the current flowing from the drain to the source. In particular, the used OTFT is characterized by a multifinger structure minimizing device size and preserving current performances.

5.1.1 Static model

In literature the behavior of the OTFT is described, generally, by the three operation regions (off, linear and saturation) of the inorganic transistor opportunely modified to take into account the specific features of the organic transistor. The equations modeling the transistor behavior obey to the Universal Mobility Law (UML) and the Variable Range Hopping (VRH) model, developed in [45]. The model has been suitably modified in [44] and the drain current flowing in the three transistor operation regions is modeled by the single equation 5.1.

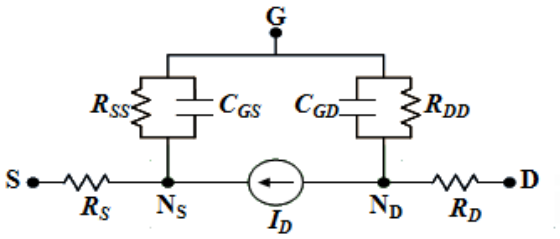

Fig. 5.2. OTFT electric scheme .

$$i_d = \mu_0 \frac{W_e}{L_e} C_{ox} \cdot (|V_{gste}|^{2m+2} - |V_{gste} - V_{dse}|^{2m+2}) \cdot (1 - \lambda V_{ds}) + I_{00} W_e \quad (5.1)$$

where

$$\mu_0 = \frac{K_3 \cdot C_{ox}^{2m}}{(2m+1)(2m+2)(2\varepsilon_0 \cdot \varepsilon_p \cdot k \cdot T)^m} \quad (5.2)$$

$$V_{gste} = \eta_i V_{th} \cdot [1 - \frac{V_{gst}}{2\eta_i V_{th}} + \sqrt{\delta^2 + (\frac{V_{gst}}{2\eta_i V_{th}} + 1)^2}] \quad (5.3)$$

$$V_{dse} = V_{sd} \cdot [1 + \frac{V_{sd}}{(\alpha_{sat} V_{gste})^m}]^{-\frac{1}{m}} \quad (5.4)$$

The coefficient K_3 is a technological parameter depending on the organic semiconductor features, k is the Boltzman constant, T is the absolute temperature. W_e is the channel width, L_e is the channel length, C_{ox} is the oxide capacitor, ε_p is the permittivity of the polymeric semiconductor, ε_0 is the permittivity of free space, m is a mobility model parameter, I_{00} is the leakage current and λ is a conductance parameter. V_{gte} and V_{dse} are effective voltages which cause the model becomes insignificant outside of their regimes of applicability.

5.1.2 Dynamic model

Some of the important low frequency circuit parameters can also be obtained from the drain current Equation 5.1. Assuming that the OTFT is an accumulation mode transistor and all of the current is due to drift and not diffusion, then the threshold voltage is defined as the gate voltage that results in an accumulation channel. The total charge on the gate electrode Q_g at any gate and drain voltage may be obtained from:

$$Q_g = -W \int_0^L C_{ox}(V_{GT} - V_x)dx \tag{5.5}$$

After some manipulations one can calculate and obtain the source-drain to gate capacitances, shown in the equation 5.6 and 5.7.

$$C_{gs} = c_t \cdot C_{gcs} \frac{(V_{gste} + v_{dec})^{2m+2}}{V_{gste} + v_{dec}} \cdot \frac{(2mm+2)V_{gdte}^{2m+3} - (2m+2)V_{gdte}^{2m+2}(V_{gste} + v_{dec}) + (V_{gste} + v_{dec})^{2m+3}}{[V_{gdte}^{2m+2} - (V_{gste} + v_{dec})^{2m+2}]^2} + C_{gs0} \tag{5.6}$$

$$C_{gd} = c_t \cdot C_{gcd} \frac{(V_{gdte} + v_{dec})^{2m+2}}{V_{gdte} + v_{dec}} \cdot \frac{(2m+2)V_{gste}^{2mm+3} - (2m+3)V_{gste}^{2m+2}(V_{gdte} + v_{dec}) + (V_{gdte} + v_{dec})^{2m+3}}{[(V_{gdte} + v_{dec})^{2mm+2} - V_{gste}^{2m+2}]^2} + C_{gd0} \tag{5.7}$$

where

$$\eta_{cs} = C_{\eta_0} + C_{\eta_{00}} V_{dse} \tag{5.8}$$

$$C_{gcd} = \frac{2m+2}{2m+3} \cdot W_e L_e C_{ox} \cdot (1 + \eta_{cs} e^{\frac{V_{gdt}}{\eta_{cs} V_{th}}})^{-1} \tag{5.9}$$

$$C_{gcs} = \frac{2m+2}{2m+3} \cdot W_e L_e C_{ox} \cdot (1 + C_{\eta_0} e^{\frac{V_{gst}}{C_{\eta_0} V_{th}}})^{-1} \tag{5.10}$$

Where V_{th} is the thermal voltage. This model and all parameters that characterize it have been implemented by using VerilogA language in CAD environment in order to design and simulate different circuits in organic technology. A deep study has been performed on extraction parameter values of OTFT model as described in Chapter 2.

5.2 All-organic conditioning circuit and peak detector design

An all-organic embedded system, composed of both organic circuitry and polymeric electromechanical devices (IP^{2}C) has been designed with the signal generation, the power supply and the conditioning circuits. A model has been implemented in CADENCE®environment to design a system that includes both the IP^{2}C sensor model and an organic peak detector schematic, able to sense the deformation of the system. The organic circuit is composed of three main blocks: sensor model, differential amplifiers, level shifter and buffers. In Fig. 5.3 a blocks schematic, composed by different circuitries, is reported.

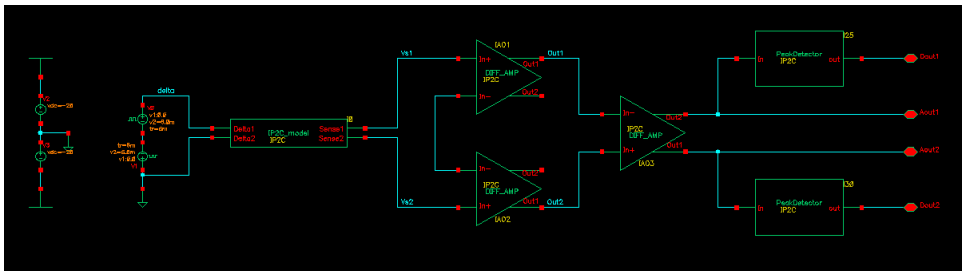

Fig. 5.3. Schematic of organic circuit for peak detection of IP^{2}C sensor.

The first part is based on the IP^{2}C sensor model, in fact using the components values of sensor equivalent model explained in Chapter 3, the organic transducer has been implemented in CADENCE environment in order to integrate it into organic technology. Fig. 5.4 shows the sensor circuit with output load implemented in order to allow its simulations.

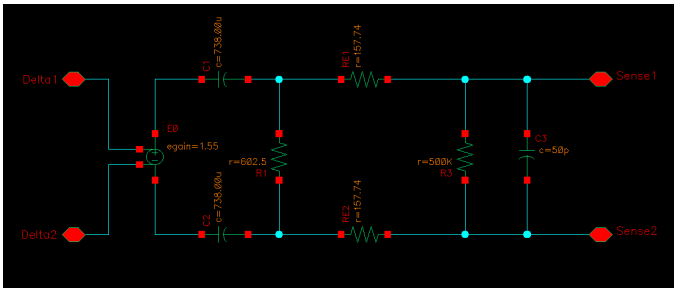

Fig. 5.4. Sensor equivalent model circuit implemented in CADENCE environment.

The second part of circuit is based on only p-type OTFTs and has been designed and tailored ad hoc for sensor model work. The first block is constituted of two differential amplifiers (Fig. 5.5). They are based on organic technology and constituted by only p-type OTFTs. Therefore all the loads in the circuit have been realized by a p-type transistor in diode configuration.

Also organic current mirror has been designed and adjusted to provide the optimum polarization current for each differential amplifier.

The last block is based on a level shifter and two output buffers (Fig. 5.6). The first device allows to obtain the required offset of signal produced by previous block. Finally, two source common configuration

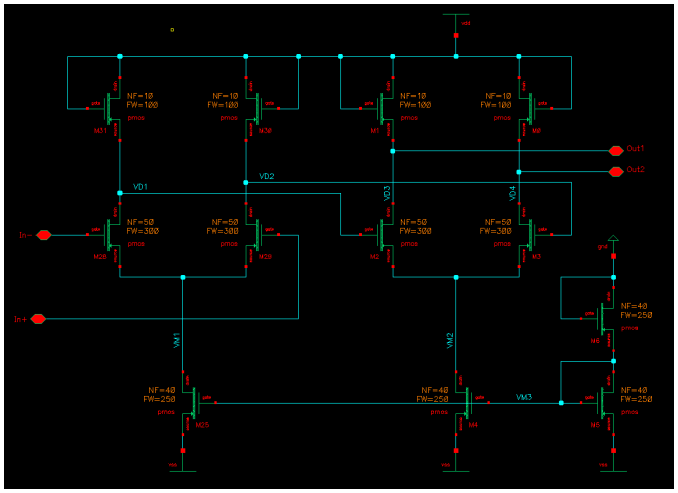

Fig. 5.5. Schematic of differential amplifier and current mirror block .

have been used as buffers. They have a specific load in order to improve static and dynamic behavior of device. They are active capacity loads that allow to overcome the limits imposed by organic technologies.

5.2.1 Circuit simulation

The whole circuit has been simulated by means of Mentor Graphics ELDO and significant signals refereing to Fig. 5.3 have been reported in Fig. 5.7.

The simulation shows that when the membrane is subjected to displacement (Delta), it produces a current slope which flows through the *RC* block. A sequence of two opposite voltage peak is detected by the differential amplifiers block producing two opposite output signal. If a negative displacement is applied, the pulse is produced at the second output. On the opposite hand, when the membrane is subjected to a positive displacement a pulse is observed at the first output. Thus

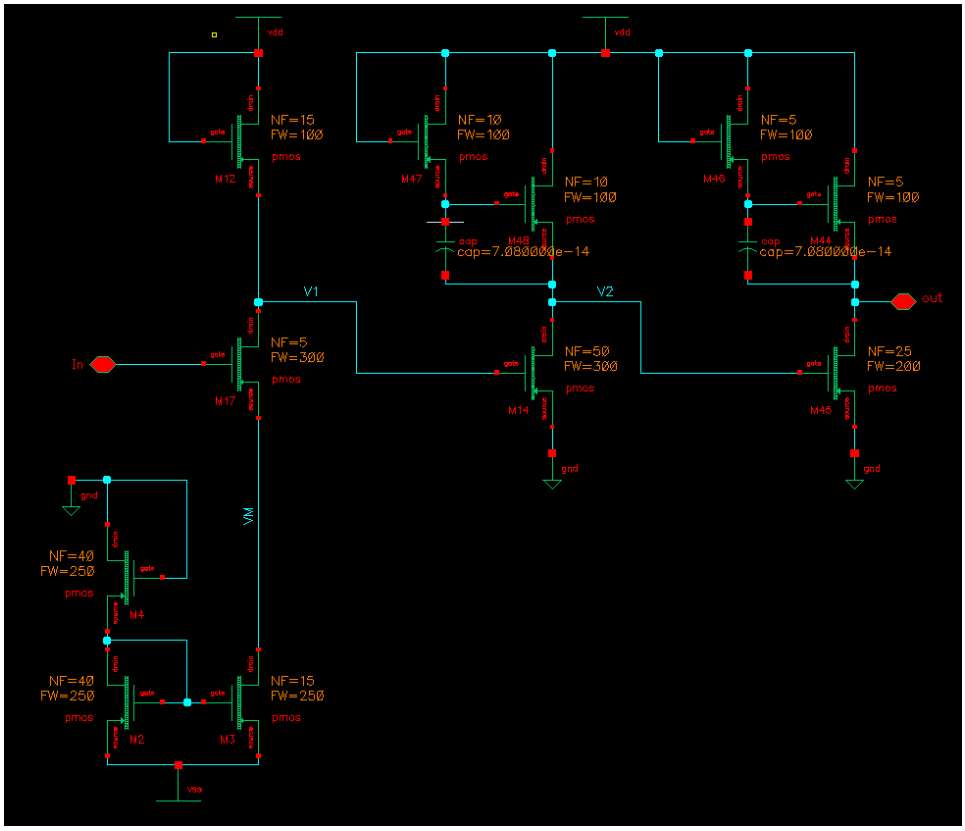

Fig. 5.6. Schematic of level shifter and buffers block.

the first or second output give an information about the displacement direction. The produced signals are well-matched with organic digital circuits which can compute the information developed by the peak detection circuit in order to obtain complex sensing information. For example, a vorticism sensor is a pressure sensor that produces an impulse in output.

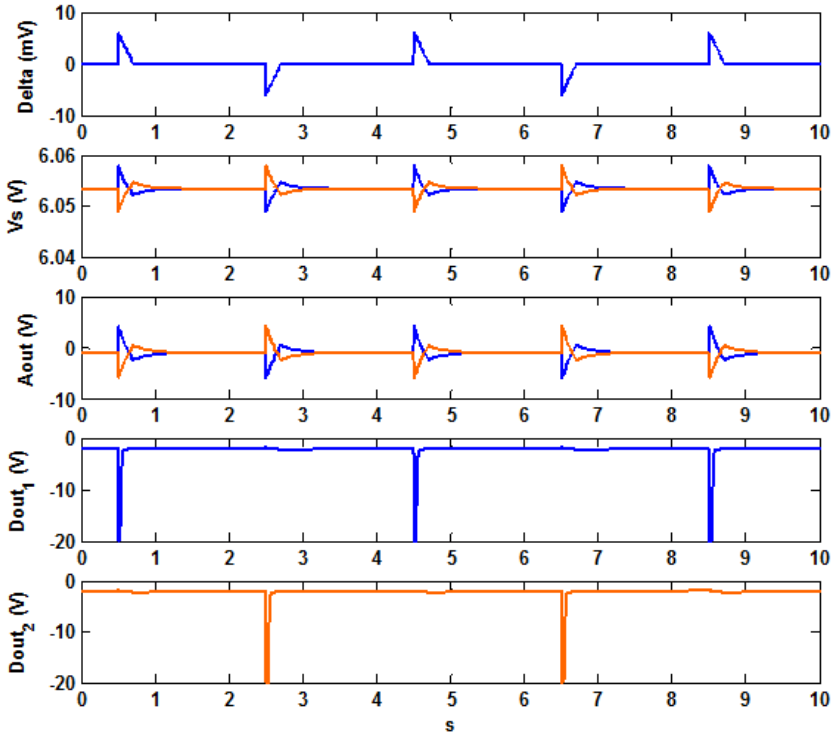

Fig. 5.7. All-organic embedded system simulation results.

5.2.2 Layout

Finally, the device layout has been realized by using Virtuoso® Layout Editor through a suitable layout design tool developed for organic technology. The Fig. 5.8 shows the circuit layout with all components, such as multifinger structures of OTFTs and capacitances. The layout has been realized with a minimum features size of $5\mu m$.

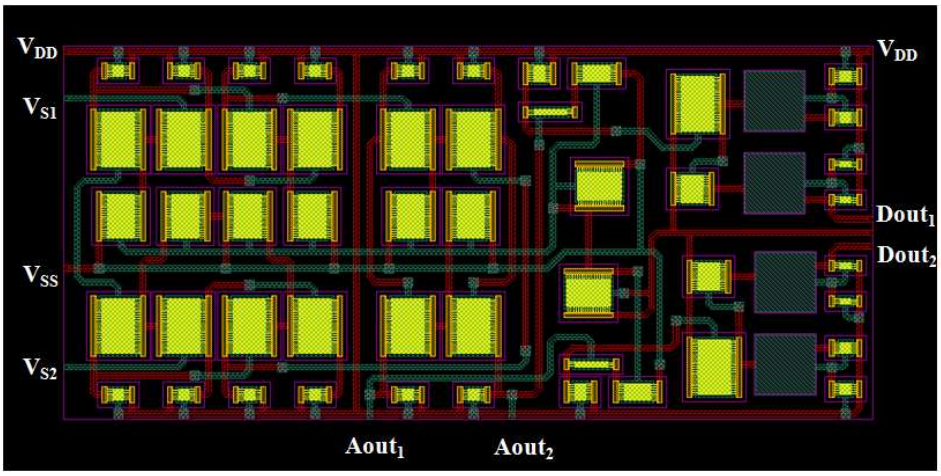

Fig. 5.8. All-Organic Embedded System layout.

5.3 Considerations

The entire design flow of an organic circuit for peak detection of polymeric transducers has been developed. Starting from models of polymeric transducer and OTFT, the design of an embedded system has been developed in organic technology. Through its simulation, every block has been analyzed and designed in order to be adapted to polymeric sensor behaviour. The circuit layout has been designed for its further realization.

Conclusions

In this work a new class of transducers has been introduced: the Ionic Polymer-Polymer Composites (IP^2Cs). These devices are polymeric membranes covered with organic conducting materials used as electrodes layers. Both sensing and actuation features have been investigated according to different manufacturing processes. The adopted devices have been integrated with organic electronics in order to design an embedded system that is composed by polymeric sensor and organic circuitry.

The investigated field is new and promising. The problems involved with the investigated topic require a lot of knowledge coming from a member of research fields. For such a reason, the activities described in this thesis are also the results of collaborations with researchers working in different fields such as chemistry material sciences and post-silicon electronics.

The analysis of IP^2Cs has been deepened in order to improve their performances both as actuator and as sensor. Starting from different organic conductors and new solvents, several transducers have been

realized and their electromechanical proprieties have been tested. The limitations imposed by organic materials have led to research of new solvents, different from water, that evaporates during functioning. The investigated solvents allow to use higher voltage values and to avoid the hydration phase that is incompatible with some organic conductors. The polymerization of EDOT on Nafion® has allowed to overcome the hydration problem, in fact the used techniques improve the adhesion of conductor to Nafion® permitting the sample soak inside solvent. In order to evaluate the IP^{2}C electromechanical proprieties several samples have been produced by Prof. Di Pasquale of DMFCI (Università degli Studi di Catania). Several experimental measurements have been performed on the produced samples which have required specifically the design and realization of a suitable measurement setup.

Research activity on organic electronics has been performed in STMicroelectonics, where different steps of a testing platform has been developed: starting from organic materials requirements and model implementation of organic thin film transistor to circuit design in CADENCE® environment. Moreover, an organic circuit has been designed in order to allow detection of peak of polymeric sensors. Starting from the models of the organic thin film transistor (OTFT) and the polymeric sensor, a tailored circuit has been designed for peak detection of an IP^{2}C motion sensor. The organic device allows to activate one of two output signals depending on the displacement direction of the sensor membrane. The circuit layout has been performed by using a specific layout design tool dedicated to organic technology developed

in STMicroelectonics.

The development of organic technologies based on organic materials consolidates the possibility to realize new devices and applications with unusual properties: flexibility, lightweight, disposability. The integration of polymeric transducers in organic circuits will allow to manufacture a very low cost and flexible device through easy deposition techniques.

It is also worth mentioning, here, that the research described in this thesis has been granted by the Italian MIUR under the national project, entitled *Innovative all-polymeric ionic transducers for post-silicon applications: realization, modeling, metrological characterization and applications*, coordinated by Prof. S. Graziani. This is an evidence of the strategic relevance of the investigated topic.

Acknowledgements

This period was for me a very important source of deeply instructive cultural and human experiences. I thank Prof. Luigi Fortuna for the opportunities that I had during my doctorate and in the STMicroelectronics laboratories and for his great helpfulness. I thank my tutor, Prof. Salvatore Graziani for being a secure and determined guide in every activity that we had. I will never forget, the support that Prof. Giovanna Di Pasquale has always given me.
Heartfelt thanks to Eng. Manuela La Rosa for the continuous support and encouragement she gave me during these years. I thank Eng. Giovanni Sicurella, Eng. Doanata Nicolosi and Eng. Alessandro Marcellino because I spent with them intense years of work and I had unforgettable experiences.

Thanks to my doctorate colleagues, Eng. Mattia Frasca and Eng. Arturo Buscarino for their friendship and their support.

A very special thanks goes to my parents and my sister for their constant support and love they give me every day.

References

1. M. Shahinpoor, Y. Bar-Cohen, T. Xue, J.O. Simpson and J. Smith,*Ionic Polymer-Metal Composites (IPMC) As Biomimetic Sensors and Actuators*, Proceedings of SPIE's 5th Annual International Symposium on Smart Structures and Materials, San Diego, 1-5 March, pp.1-17 (1998).
2. M. Shahinpoor, K. J. Kim, *Ionic polymer-metal composites: I. Fundamentals*, Smart Materials and Structures, Vol. 10, pp. 819-833 (2001).
3. C. Bonomo, L. Fortuna, P. Giannone, S. Graziani, S. Strazzeri, *A model for ionic polymer metal composites as sensors*, Smart Materials and Structures, Vol.15, pp.749-758 (2006).
4. C. Bonomo, L. Fortuna, P. Giannone, S. Graziani, S. Strazzeri, *A nonlinear model for ionic polymer metal composites as actuators*, Smart Materials and Structures, Vol.16, pp.1-12 (2007).
5. E. Malone, H. Lipson, *Freeform Fabrication of Ionomeric Polymer-Metal Composite Actuators*, Rapid prototyping Journal, Vol.12, Issue5, pp.244-253 (2006).
6. L. Fortuna, S. Graziani, M. La Rosa, D. Nicolosi, G. Sicurella and E. Umana "Modelling and Design of All-Organic Electromechanic Transducers", European Physical Journal - Applied Physics (EPJ-AP) , Vol.46, pp. 12512 (2009).
7. G. Di Pasquale, L. Fortuna, S. Graziani, M. La Rosa, D. Nicolosi, G. Sicurella, E. Umana, *All-Organic Motion Sensors: Electromechanical Modeling*, IEEE Transaction on Instrumentation and Measurement (I2MTC'08 Special Issue), 58, Issue 10, pp. 3731 - 3738 (2009).

8. I. M. Ward and J. Sweeney, *An Introduction to the Mechanical Properties of Solid Polymers* second edition, John Wiley & Sons (2004).
9. L. Fortuna, S. Graziani, M. La Rosa, D. Nicolosi, G. Sicurella and E. Umana, *Modelling and Design of All-Organic Electromechanic Transducers*, European Physical Journal - Applied Physics (EPJ-AP), Vol.46, no.1, pp.12513 p1-p4 (2009).
10. E. Ebisawa, T. Kurokawa,, S. Nara, *Electrical properties of polyacetylene/polysiloxane interface* J. Appl. Phys. Vol. 54, pp.3255-3260 (1983).
11. H. Hoppe, N. S. Sariciftci, *Organic solar cells: An overview*, J. Mater. Res., Vol. 19, no. 7, pp.1924-1945 (2004).
12. L. Torsi, A. Dodabalapur, *As plastic analytical sensors*, Analytical Chemistry,Vol.77, pp.381-387, (2005).
13. J. Jang, *Displays develop a new flexibility*, Materials Today, Vol.9, no 4, pp.46-52, 2005.
14. B. S. Ong, ,Y. Wu, P.Liu, S. Gardner, *High-performance semiconducting polythiophenes for organic thin-film transistors*, J. Am. Chem. Soc. Vol. 126, pp.3378-3379, 2004.
15. C. Bailey, K. Genevicius, M. Shkunov, D. Sparrowe, S. Tierney and I. McCulloch,*Stable polythiophene semiconductors incorporating thieno[2,3-b]thiophene*, J. Am. Chem. Soc. 127, pp.1078-1079 (2005).
16. I. McCulloch, M. Heeney, C. Bailey, K. Genevicius, I. MacDonald, M. Shkunov, D. Sparrowe, S. Tierney, R. Wagner, W. Zhang, M. L. Chabinyc, R. J. Kline, M. D. McGehee and M. F. Toney,*Liquid-crystalline semiconducting polymers with high charge-carrier mobility*, Nature Materials, Vol. 5, pp.328-333 (2006).
17. J. Ouyang, Q. Xu, C. Chu, Y. Yang, G. Li, J. Shinar, *On the mechanism of conductivity enhancement in poly(3,4-ethylenedioxythiophene):poly(styrene sulfonate) film through solvent treatment*, Polymer, 45, pp.8443-8450 (2004).
18. $http://www.hcstarck.com/medien/dokumente/document_21_clevios_high_web.pdf$
19. Y. Xia, G. M. Whitesides, *Replica molding with a polysiloxane mold provides this patterned microstructure*, Angew. Chem. Int. Ed.,Vol. 37, pp.550-575 (1998).
20. C.M. Sotomayor Torres, S. Zankovych, J. Seekamp, A.P. Kam, C. Clavijo Cedenõ, T. Hoffmann, J. Ahopelto, F. Reuther, K. Pfeiffer, G. Bleidiessel, G. Gruetzner, M.V. Maximov, B. Heidar, *Nanoimprint lithography: an alternative nanofabrication approach*, Materials Science and Engineering: C, Vol. 23, pp.23-31 (2003).

21. L. Fortuna, M. Frasca, M. La Rosa, G. Sicurella, E. Umana, *Organic Chuas Circuit*,International Journal of Bifurcation and Chaos, Vol. 17, No.9, pp. 3035-3045 (2007).
22. M. La Rosa, D. Nicolosi, L. Occhipinti, G. Sicurella,L. Fortuna, E. Umana, *Modelling of organic thin film transistor* ICOE 08, Eindhoven, (2008).
23. L. Fortuna, M. Frasca, M. La Rosa, L. Occhipinti, G. Sicurella, E. Umana, *Nonlinear electronic circuits through organic transistors*", in Proc. of International Conference on Organic Electronics '06 (2006).
24. H. Shirakawa, E. J. Louis, A. G. MacDiarmid, C. K. Chiang and A. J. Heeger, *Synthesis of electrically conducting organic polymers: halogen derivatives of polyacetylene, (CH)x*, J. Chem. Soc., Chem. Commun., pp.578 - 580 (1977).
25. T. Pompe, A. Fery, and S. Herminghaus, *Submicron contact printing on silicon using stamp pads*, Langmuir 15, pp.2398-2401 (1999).
26. A.R. Brown, D.M. de Leeuw, E. E. Havinga and A. Pomp, *A universal relation between conductivity and field-effect mobility in doped amorphous organic semiconductors*, Synth. Met, Vol. 68, pp.65-70 (1994).
27. D. Natali, L. Fumagalli, M. Sampietro, *Modeling of organic thin film transistor: Effect of compact resistances*, Journal of applied physics, Vol. 101, 014501 (2007) .
28. Gabrielli Claude, *Use and applications of electrochemical impedance techniques* Solartron Part - Issue B: April 1997, 12860013(1997).
29. Di Pasquale G., Fortuna L., Graziani S., La Rosa M., Umana E., *A study on IP2C actuators using ethylene glycol or EmI-Tf as solvent*, Smart Materials and Structures (submitted).
30. Barbar J. Akle, Matthew D. Bennett, Donald J. Leo , *High-strain ionomeric-ionic liquid electroactive actuators*, Elsevier, Sensors and Actuators A, Vol. 126, pp. 173-181 (2006)
31. M. Döbbelin, R. Marcilla, M. Salsamendi, C. Pozo-Gonzalo, P.M.Carrasco, J.A. Pomposo, D.Mecerreyes, *Influence of Ionic Liquids on the Electrical Conductivity and Morphology of PEDOT:PSS Films*, Chem. Mater., Vol. 19, 2147-2147 (2007).
32. X. Crispin, F.L.E.Jacobsson, A.Crispin, P.C.M.Grim, P.Andersson, A.Volodin, C.van Haesendonck, M.Van der Auweraer, W.R. Salaneck, M.Berggren, *The Origin of the High Conductivity of Poly(3,4-ethylenedioxythiophene)-Poly(styrenesulfonate) (PEDOT-PSS) Plastic Electrodes*, Chem. Mater., Vol. 18, pp. 43544360 (2006)

33. Sia Nemat-Nasser and Shahram Zamani, *Experimental Study of Nafion- and Flemion-based Ionic Polymer metal Composites (IPMCs) with Ethylene Glycol as Solvent*, Smart Structures and Materials 2003: Electroactive Polymer Actuators and Devices, SPIE, Vol. 5051, pp.233-244 (2003).
34. David R. Lide,*CRC Handbook of Chemistry and Physics*, CRC Press LLC, 2001.
35. http://www.ec.gc.ca/lcpe-cepa/default.asp?lang=En&n=24240347-1&offset=6
36. A.B. McEwen, H.N. Ngo, K. LeCompte, J.L. Goldman, *Electrochemical properties of imidazolium salt electrolytes for electrochemical capacitor applications*, J. Electrochem. Soc., Vol. 146, pp. 1687-1695 (1999).
37. W. Lu, A.G. Fadeev, B. Qi, E. Smela, B.R. Mattes, J. Ding, G.M. Spinks, J. Mazurkiewicz, D. Zhou, G.G. Wallace, D.R. MacFarlane, S.A. Forsyth, M. Forsyth, *Use of ionic liquids for conjugated polymer electrochemical devices*, Science, Vol. 297, pp. 983-987 (2002).
38. $http : //www.sigmaaldrich.com/catalog/ProductDetail.do?D7 = 0\&N5 = SEARCH_CONCAT_PNO\%7CBRAND_KEY\&N4 = 04367\%7CFLUKA\&N25 = 0\&QS = ON\&F = SPEC$
39. http://www.clevios.com/medien/datenblaetter/pd-6072_3.pdf
40. P.Lee-Sullivan, D. Dykeman, *Guidelines for performing storage modulus measurements using the TA Instruments DMA 2980 three-point bend mode: I. Amplitude effects*, Polym.Test., Vol.19,pp. 155-164(2000)
41. K.M. Newbury, *Characterization, modeling, and control of ionic polymer transducers*, PhD Dissertation Virginia Tech. etd-09182002-081047(2002).
42. Simon J. Higgins, Keith V. Lovell, R. M. Gamini Rajapakse and Nadia M. Walsby, *Grafting and electrochemical characterisation of poly-(3,4-ethylenedioxythiophene) films, on Nafion and on radiation-grafted polystyrenesulfonate-polyvinylidene fluoride composite surfaces* , J. Mater. Chem., Vol.13, 2485 - 2489 (2003).
43. Gamota D. R., Brazis P., Kalyanasundaram K. and Zhang J., *Printed Organic and Molecular Electronics*, Kluwer Academic Publishers (2004).
44. M. Fadlallaha, G. Billiota, W. Ecclestonb and D. Barclayc, *DC/AC unified OTFT compact modeling and circuit design for RFID applications*, Solid-State Electronics, Vol. 51, Issue 7, pp. 1047-1051 (2007).

45. A.R. Brown, D.M. de Leeuw, E. E. Havinga and A. Pomp, *A universal relation between conductivity and field-effect mobility in doped amorphous organic semiconductors*, Synth. Met, vol. 68, pp.65-70 (1994).

List of Figures

List of Tables